# Micelle-core/chitosan-shell (chito-micelles) enriched with gamma oryzanol: physical-chemical features, safety, translational nephroprotective potential and emphasis on sirtuin-1 associated machineries

*Enas Elmowafy*[1], *Marwa Omar El-Derany*[2], *Luca Casettari*[3], *Mahmoud E. Soliman*[1,4*] *and Riham I. El-Gogary*[1]

[1]*Department of Pharmaceutics and Industrial Pharmacy, Faculty of Pharmacy, Ain Shams University, Cairo, Egypt,*
*Monazzamet Elwehda Elafrikeya Street, Abbaseyya, Cairo, Egypt, 11566*

[2]*Department of Biochemistry, Faculty of Pharmacy, AinShams University, Cairo, Egypt,*
*Monazzamet Elwehda Elafrikeya Street, Abbaseyya, Cairo, Egypt, 11566*

[3]*Department of Biomolecular Sciences, University of Urbino Carlo Bo, Piazza delRinascimento, 6, 61029 Urbino (PU), Italy.*

[4]*Egypt-Japan University of Science and Technology (EJUST), New Borg El Arab, Alexandria 21934, Egypt*

*** Corresponding author:**
*Mahmoud E. Soliman*
Department of Pharmaceutics and Industrial Pharmacy,
Faculty of Pharmacy, Ain Shams University, Cairo, 11566, Egypt
Tel.: +2 01005164052 Fax: +20 2 0224011507.

Email: mahmoud.e.soliman@pharma.asu.edu.eg

**Abstract**

Gamma oryzanol (ORZ) is a nutraceutical that is poorly water soluble with poor intestinal absorption. In the current work, ORZ was nanoformulated into uncoated and chitosan coated micelles based on methoxy-poly(ethylene glycol)-b-poly(ε-caprolactone) (mPEG-PCL) and poly(ε-caprolactone)-b-methoxy-poly(ethylene glycol)-b-poly(ε-caprolactone) (PCL-PEG-PCL) copolymers for augmenting ORZ oral delivery. The physicochemical properties, morphological study, in-vitro release and safety of the nanoplaforms were determined. Importantly, the nephroprotective competence of the nanoplaforms was analyzed against acute kidney injury (AKI) rat model and the sirtuin-1 associated machineries were assessed. The results revealed that the micelles exerted particle size (PS) from 97.9 to 117.8 nm that was markedly increased after chitosan coating. The reversal of zeta potential from negative to highly positive further confimed efficient coating. *In vitro* release profiles demonstrated prolonged release pattern which followed Higushi model. The nanoforms conferred higher cell viability values than free ORZ on vero cell line. The designed micelles displayed augmented nephroprotection compared to free ORZ with the supremacy of chitosan coated micelles over uncoated ones in restoring kidney parameters to normal levels. The attenuated AKI was fulfilled via the modulation of sirtuin-1 signaling pathways translated by restoring the histological features, increasing renal antioxidant states, renal autophagy and decreasing renal inflammation and renal apoptosis. These outcomes confirmed that surface modification with chitosan had a considerable leverage on micelles safety, release behavior and in vivo performance.

**Keywords**

Oral delivery; gamma oryzanol;polymeric micelles; chitosan; nephroprotection; sirtuin-1

## 1. Introduction

In recent years, the occurrence of nephrotoxicity associated with unrationalized extensive dosing of some drugs or as an adverse toxic effect of various drugs like antibiotics, anticancers and other chemicals like pesticides has increased extensively. Moreover, kidney exposure to chemicals such as glycerol or adenine leads to nephrotoxicity (Adedapo et al., 2021; Al-Okbi et al., 2019; Azab et al., 2017; Song et al., 2021; Wu and Huang, 2018). The pathogenesis of kidney failure following exposure to these causative agents, especially glycerol, usually involves increased serum levels of urea, creatinine and blood urea nitrogen. Moreover, a decrease in renal blood flow in addition to liberation of myoglobin from muscles into the blood stream occurs resulting in the production of reactive oxygen species (ROS), lipid peroxidation and acute tubular necrosis (ACT) which contributes further to inflammatory process, fibrosis and apoptosis consequently resulting in alteration and loss of renal function and further complications such as diabetes and stroke. Sirtuin-1 is known to play a central protective role against AKI. Sirtuin-1 has been proved to inhibit cell apoptosis induced by oxidative stress and inflammation. Interestingly, sirtuin-1 was found to be an important regulator of renal cell autophagy. Whereas, reduced sirtuin-1 levels were proved to be crucial in the aging of the kidneys through the deacetylation and the activation of some transcription factorswhich subsequentlyreduce ATG-mediated autophagy.It has been proposed that convalescence from kidney dysfunction can be achieved through prophylactic and/or early therapeutic administration of antioxidant and / or anti-inflammatory drugs. Among the powerful candidates proposed for this aim are the nutraceuticals owing to their reported antioxidant, anti-inflammatory and lipid lowering effects(Adedapo et al., 2021; Al-Okbi et al., 2019; Song et al., 2021).

Gamma oryzanol (ORZ) is a major component isolated from rice bran. Several studies reported its several beneficial therapeutic activities. It is reported to have powerful antioxidant, anticancer, anti-inflammatory, lipid lowering and neuroprotective effects owing to its transferulic acid esters components which accounts for 80% of its composition(Al-Okbi et al., 2019; Rawal et al., 2018; Ruktanonchai et al., 2009; Viriyaroj et al., 2009; Yang and Chiang, 2019).

Recent attention was directed toward investigating the protective effects of gamma ORZ against multiple kidney diseases. **Al-Okbi et al., 2020** proved the protective effect of ORZ on the kidney and liver against CVD and hepatocellular carcinoma(Al-Okbi et al., 2019). However, the underlined molecular mechanism for the therapeutic effects of ORZ in acute kidney injury is still

far from clear and the effect of ORZ on sirtuin-1 signaling pathway hasn't been yet discovered. But unfortunately, the clinical application of ORZ is hampered by its low water solubility, poor bioavailability and rapid metabolism. To overcome ORZ solubility and stability problems, several studies formulated ORZ in various nanoforms such as; liposomes, niosomes, solid lipid nanoparticles, ethylcellulose polymeric nanoparticles, penetration enhancer vesicles (PEVs), self-emulsifying alginate beads & chitosan nanoparticles (Aldalaen et al., 2020; Ghaderi et al., 2014; Manosroi et al., 2012; Rawal et al., 2018; Seetapan et al., 2010; Viriyaroj et al., 2009; Yang and Chiang, 2019). Furthermore, ORZ encapsulation in a nanosystem would exploit from the diverse advantages of nanodelivery systems such as enhancing better delivery of the drug to target site(Rawal et al., 2018).

Among the most promising nanocarriers emerging are the polymeric micelles. Their amphiphilic core-shell structure confers the encapsulation of hydrophobic drugs in their cores besides the hydrophilic stabilizing parts forming the shell eventuating a robust platform that could enhance drug solubility and targetability hence its therapeutic action. Moreover, the hydrophilic shell has been reported to minimize protein adsorption on micelles hence eluding the uptake by the reticuloendothelial system (RES) hence enhancing the drug's bioavailability(Aboud et al., 2020; Ahmad et al., 2014; Gong et al., 2010; Hou et al., 2019; Zhang et al., 2018). Previously our group reported the formulation of the hydrophobic drug,methizolamide into diblock copolymer; mPEG-PCL micelles which showed enhancement in its therapeutic efficacy(Elmowafy et al., 2019).

Further extension to this work, herein we utilized DB and TB copolymers self-organized into micelles for maneuvering biopharmaceutical performance of the poorly water-solublenutraceutical ORZ. Intestingly, some studies reported that further coating of nanocarriers with polymers such as Eudragit® RS 100 or CS could enhance their biocompatibility, bioadhesivity and stability(Cheng et al., 2019). Therefore, a complimentary approach of decorating the micelles with a highly biocompatible polymer such as chitosan (CS), has been attempted. This would probably enhance the biocompatibility, increase the stability, mucoadhesivity of the nanosystem(Rawal et al., 2018). Furthermore, the incorporation of CS in the nanosystem has been reported to augment epithelial permeability through enhancing contact with cell membrane and opening occlusion areas (de C Coelho Junior et al., 2021).

To the best of our knowledge, the formulation of ORZ in polymeric copolymeric micelles with or without CS coating and its in-vitro and in-vivo evaluation for nephroprotection against glycerol induced AKI hasn't been attempted in any other study so far. Therefore, in this light, the aim of the present study was to optimize the formulation parameters of polymeric micelles of ORZ including colloidal size, reasonable entrapment, sustained release pattern, and a promising safety profile. A comparative study was performed between di-block and tri-block PCL polymers with respect to their effect on physicochemical attributes of micelles, drug release and solid state analyses.The effect of micelles coating with CS on thephysicochemical properties of the micelles was studied. In addition, the prophylactic potential of the prepared systems on the in-vivo glycerol induced AKI in rat and sirtuin-1 associated machineries were studied.

## 2. Materials and Methods

### 2.1Materials

mPEG-PCL di-block and tri-block copolymers with respective molecular weight ($M_w$) of 4000 and 5000 Da were synthesized in our lab using methoxy-PEG (mPEG) 1.9 kDa and ε-caprolactone, purchased from Polysciences (Germany) and Sigma-Aldrich (Italy), respectively. Oryzanol(ORZ) was purchased from Bulkactivescompany,Taiwan.Chitosan (CS), viscosity 9 cPwas kindly supplied by Primex, Iceland.Sodiumhydroxide, potassiumdihydrogen phosphate, tween 80, chloroform and methanol were supplied from El-Nasr Pharmaceutical Co., (Egypt).Vero cells (ATCC®CCL-81™) were obtained from American Type Culture Collection, (Manassas, VA, USA). Porcine mucin type II, MTT (3-(4,5-dimethylthiazol-2-yl)-2,5-diphenyl-tetrazolium bromide) and DPPH werepurchased from Sigma-Aldrich Co. (St Louis, MO, USA). Spectra/Pordialysismembrane (molecular weight cutoff 12–14 kDa) was purchased from Spectrum Laboratories (Canada).

### 2.2 Synthesis and characterization of the copolymers.

Synthesis and characterization of mPEG-PCL and PCL-mPEG-PCL were performed by the ring opening polymerization (ROP)technique and $H^1$-NMR and GPC analysis respectively as previouslydescribed by our group(Elmowafy et al., 2019; Shalaby et al., 2016; Shalaby et al., 2014).

### 2.3 Preparation of micelle-core

ORZloaded micelle-corewas prepared using a modified thin film hydration method as stated previously(Elmowafy et al., 2019). In brief, pegylated PCLcopolymer,was weighed into a round bottom flask and dissolved in chloroform:methanol mixture (3:2 v/v) with the aid of sonication at 25°C. Subsequently, ORZ was dissolved in the copolymer solution, at polymer to drug ratios of 5:1 and 10:1 w/w. the organic solvents were removed using a rotary evaporator (HB4-basic, IKA, Germany) under the following conditions: rotation speed 200 rpm, rotation time 30 min and temperature 60°C till the formation of a thin film of dry drug-polymer mixture. Hydration of the obtained film was performed through the addition of Milli-Q water (10 mL) followed by rotation for an additional 30 min. the micelles were filtrated using a 0.2 µm cellulose acetate membrane filter to remove the unincorporated drug aggregates(Patra et al., 2018).The formulations were sealed in clean glass vials and stored under cool conditions at 4°C. The composition of the ORZ micelle-core is presented in Table 1.

**2.4. Dimensional characterization**

Colloidal parameters (micelle size (MS), polydispersity index (PDI) and zeta potential (ZP)) were measured at 25˚C by diluting micelles with deionized water using a Zetasizer(Zetasizer;Malvern Instruments, Malvern, UK).

**2.5. Determination of ORZ percentage entrapment efficiency (EE%) and percentage drug loading (DL%)**

The quantity of ORZ encapsulated within the micelle-core was determined after filtration of the micelles using 0.22 µm filters to remove the unentrapped drug. The percentage entrapment efficiency (% EE) of ORZwas estimated as previously reported(Aldalaen et al., 2020). The amount of ORZ entrapped in the micelles was calculated after micelles disruption by methanol, in which 100 µL of micelles were mixed with 10 ml of methanol.The drug was measured spectrophotometrically at 319 nm using a UV–Visspectrophotometer (Shimadzu, model UV-1601 PC, Kyoto, Japan).The amount of ORZwas then determined according to a calibration curve of ORZ inmethanol.

The % EE and % DL of ORZ wereestimated using the following equations(Kumar et al., 2020):

$$EE\% = \frac{\text{Weight of loaded ORZ in micelles}}{\text{Theoritical Weight of ORZ added}} \times 100 \quad (1)$$

$$DL\% = \frac{\text{Weight of loaded ORZ in micelles}}{\text{Weight of copolymer}} \times 100 \quad (2)$$

**2.6.Preparation and characterization of micelle-core/ chitosan shell nano-carriers (chito-micelles)**

The selected micelle-core formulations were coated using different concentrations of CS solution (1% acetic acid), namely 0.25, 0.5 and 1% w/v. In brief, an aqueous solution of CS was added to the formed micellardispersion to achieve a micelles: CS coat ratio of 1:1 v/v, and stirred for 30 min at room temperature. The MS, PDI and ZP of the formed chito-micelles were measured using a Zetasizer.

**2.7. Morphological examination**

Morphological examination of the selected micelle-core and chito-micelleswas done using a high-resolution transmission electron microscope (HR-TEM)(Jeol Electron Microscope, JEM-1010, Japan). A droplet of the suspension was added to a carbon film-covered copper grid without staining. Excess liquid was drained with the aid of a filter paper. After sample dryness, PMs were visualized under an electron beam at a voltage of 200 kV.

**2.8. *In vitro* release characteristics and kinetics in simulated intestinal fluid (SIF)**

The extent of ORZ release from the selected micelle-core, chito-micellesand ORZethanolicsolutionwas carried out using a membrane diffusion technique(El-Gogary et al., 2022; Elmowafy et al., 2020; Elmowafy et al., 2019). An aliquot of the selected formulationsor drug solution equivalent to 1 mg of ORZ was placed in the dialysis membrane. The dialysis bag was then immersed in vials containing 100 mL of the dissolution medium (simulated intestinal fluid (SIF) containing 0.5% w/v tween 80; pH 6.8) maintained at 37 °C in a shaking incubator at 50 rpm. At predetermined time points over a 24 h period, 1 mL aliquots were withdrawn and the same volume of fresh SIF was added back to the vials. ORZconcentration was determined by UV spectrophotometry (UV-1601 PC, Shimadzu, Kyoto, Japan) at 319 nm. Kinetics of drug release were studied by plotting data obtained from in vitro release in various kinetic models viz. first order, zero order, and Higuchi. Mechanism of drug release was assessed by Peppas model.

**2.9. Solid state characterization**

### 2.9.1. Differential scanning calorimetry (DSC)

The thermal properties of ORZ, DB and TB mPEG-PCL copolymer, selected lyophilized micelle-core formulations and their corresponding chito-micelles "freeze dried using Christ, alpha 1-2 LD plus, Germany),were studied using DSC (Shimadzu-DSC 60, Japan). Powdered samples (2-3 mg) were sealed in aluminum pans with lids and scanned at a temperature between 0 and 300°C at a rate of 10°C/min, using dry nitrogen as a carrier gas with a flow rate of 25 mL/min (Gad et al., 2022; Lamie et al., 2022).

### 2.9.2. FT-IR characterization

FT-IR spectra of ORZ, DB and TBmPEG-PCL copolymer, selected lyophilized micelle-core formulations and their corresponding chito-micelles were recorded in the range of 4000-400 $cm^{-1}$ on a Nicolet 6700 FTIR (Thermo Scientific, USA). Powdered samples were loaded on KBr discs without special treatment. All spectra were recorded at a resolution of 4 $cm^{-1}$ and 16 scans at ambient temperature.

### 2.10.Colloidal stability study

The colloidal stability of the selectedchito-micelles was tracked over time using assessments of physical parameters (PS, PDI, and ZP). The stability experiments were continued for a period of 30 days, during which the micelles were stored in the refrigerator at4˚C.

### 2.11. Suitability of chito-micelles for oral delivery

### 2.11.1. Stability of chito-micelles in simulated intestinal fluid (SIF)

The physical stability of the selectedchito-micelles was evaluated in intestinal conditionsas reported earlier(Kumar et al., 2020). The chito-micelles were added into SIF and incubated for 6 h at 37 ◦C(Ji et al., 2018). Subsequent to incubation, chito-micelles were collected and measured for their PS and PDI by using a zeta-sizer.

### 2.11.2. Mucoadhesion

The *in vitro* mucin assay was conducted to investigate the interaction between mucin and the prepared chito-micelles as described previously with slight modification (Kengkittipat et al., 2021)**.** Briefly, porcine mucin was dissolved in SIF (0.1% w/v). The mucin solution was then centrifuged at 4000 rpm for 20 min. Then the mucin solution was added to

chito-micelles and uncoated micelles at1:1 v/v ratioand incubated at 37 ◦C for 1 h.MS and ZPwere assessed by using dynamic light scattering.For comparison, the corresponding micelle-core was also investigated under the same condition.

### 2.12. **Comparative*In vitro*antioxidant potential**

DPPH free radical scavenging assay was conducted in order to elucidate the antioxidant activity of the encapsulated ORZ in the selectedchito-micelles (C-$M3_{(0.5)}$) and the corresponding micelle-core (M3) as previously described(Aslam et al., 2020)**.**The freshly prepared DPPH solution (0.1 mM) was added to the selected formulations(500µg/mL) separately and incubated for half an hourat room temperature. the absorbance of the solution was then determined at 517 nm and % inhibition of DPPH was measured. Ascorbic acid was used as a standard antioxidant.

### *2.13. In vitro* **cytocompatibility**

In order to assess the nephroprotective effects of ORZ and micelle-core and chito-micelles on African Green Monkey Kidney (vero cells), their mitochondrial dehydrogenase activity was demonstrated using MTT procedure as described elsewhere(Tentor et al., 2017).

### **2.14. In-Vivo nephroprotectionexperiment**

The efficacy of the selected chito-micelles (C-$M3_{(0.5)}$) and the corresponding micelle-core (M3) in preventing nephotoxicity following their oral delivery was evaluated using Wistar albino rats. The results were compared to the effect of ORZ suspension (prepared via dispersion of ORZ in carboxymethyl cellulose solution (0.5%)).

#### **2.14.1. Animals**

Thirty male Wistar albino rats (180-200 g) were used. All rats were supplied with a standard chow diet and drinking water during the experiment and were caged in open cages at 25 °C with 12 h light and dark cycles at the animal facility of the Faculty of Pharmacy (Ain Shams University, Egypt). This in-vivo study was approved by the Ethics Committee at the Faculty of Pharmacy, Ain shams university, Egypt.

#### **2.14.2. Experimental design and induction of acute kidney injury (AKI) model**

All rats were left for one week for acclimatization before starting the experiment. The experimental model duration was seven days. Rats were dividedinto five groups (6 rats per group) as follows:

Group I received normal saline orally (normal control)

Group II received IM glycerol solution (positive control)

Group III received ORZ suspension

Group IV received ORZ micelle-core

Group V received ORZ chito-micelles

AKI was induced based on Adedapo et al., work(Adedapo et al., 2021).

For groups (III-V), 1 mL dose of ORZ preparations (50 mg/kg ORZ) was administered via oral gavage. At the end of the experimental duration, 24 h after glycerol administration, blood samples were collected from the retro-orbital plexus. Then, serum was separated by cold centrifugation of the clotted blood at 4000 rpm for 20 min and then serum was aliquoted and stored at −80°C for its subsequent use in biochemical tests. Kidney tissues were dissected and washed with ice-cold saline and stored at −80°C for thesubsequent molecular analysis or fixed in 10% neutral formalin for histopathological examinations.

### 2.14.3. Assessment of nephrotoxicity indices

The kidney function markers; serum concentrations of urea and creatinine were determined spectrophotometrically using a colorimetric assay byusing available commercial kits (Biodiagnostics, Cairo, Egypt).

## 2.15. Histopathological assessment and scoring of treated renal tissues

Kidney tissues were fixed in 10% neutral buffered formalin for 72 h. Then, kidney tissues were trimmed and added in serial grades of ethanols, cleared in xylene, and embedded into Paraplast tissue embedding media. Then, blocks were prepared and cut by rotatory microtome into 4μm thick tissue sections. Tissue sections were stained by Hematoxylin and Eosin (H&E) and examined(Gad et al., 2022; Tiboni et al., 2022).

Microscopic scoring was done as previously described blindly by the same pathologist. All light microscopic examination and scoring data were obtained by using the Leica Application module for histological analysis attached to Full HD microscopic imaging system (Leica Microsystems GmbH, Germany).

## 2.16. Sirtuin-1 signaling pathway and associated machineries

### 2.16.1. Reverse transcription-quantitative real-time polymerase chain reaction(RT-qPCR)

Extraction of total RNA was done using triazol. One µg total RNA was reversibly transcribed into cDNAusing high-capacity cDNA Synthesis Kit (Thermo Scientific co., USA). qRT-PCR was performed using power up SYBR (Applied Biosystems) utilizing an ABI 7500 RT-PCR System (Applied Biosystems, Foster City, CA, USA). Sequences of PCR primer pairs are shown in **Table 2**. Fold change for the studied mitochondrial antioxidant genes including manganese superoxide dismutase (MnSOD), uncoupling protein-2 (UCP2) and peroxisome proliferator-activated receptor gamma coactivator 1-alpha (PGC-1α) genes, Autophagy-related genes (ATG 5, 7 and 12) and unc-51 like autophagy activating kinase 1 (ULK1), apoptotic genes as B-cell lymphoma 2 (Bcl-2), Bcl-2 Associated X (Bax), p53 and p53 upregulated modulator of apoptosis (PUMA) genes were determined and normalized to β-actin gene as a reference gene. The relative quantification was then calculated by the expression $2^{-\Delta\Delta Ct}$ .

### 2.16.2. Protein assessment by ELISA

Renal homogenate was washed and homogenized in cold phosphate buffer saline (PBS) buffer then, centrifuged for 20 min at 4,000 rpm at 4 °C, and supernatant was collected. The total proteins of the homogenate were quantified using a bicinchoninic acid (BCA) assay kit Sigma-Aldrich (St Louis, MO, USA). Renal assessment of IL-6, IL-1β and TGF-β was conducted in renal tissue homogenate using ELISA assay kits (Bioassay, Biotech, CO., Ltd Hangzhou, China),All ELISA procedures were done by Hyprep Automated ELISA system (Hyperion Inc, Miami, FL) according to the manufacturer's instructions.

### 2.17. Statistical analysis

All data were expressed as the mean of 3 replicates ± SD. The data obtained were compared using one-way analysis of variance (ANOVA) and the significance of the difference between formulations was calculated by Tukey-Kramer multiple comparisons using Graph Pad Instat®software(GraphPad Software, California).

In vivo data were expressed by mean ±SEM. Statistical significance was estimated by One-way ANOVA followed by Tukey's Post Test. $P< 0.05$ was considered to be statistically significant. The IBM SPSS statistics (V.19.0, IBM Corp., USA, 2010) was used for in vivo data analysis.

## 3. Results and discussion

In this study we synthesized both DB (mPEG–PCL) and TB (PCL-PEG-PCL) copolymers to prepare self assembling micelles for entrapment of ORZ in a comparative manner. Poor

solubility and intestinal absorption of ORZ leads to limited bioavailability. Therefore, this work investigated different micelles prepared from DB and TB copolymers, in an attempt to increase ORZ bio distribution and efficacy. Refer to literature, particle size and drug release profile of the prepared micelles were well related to the copolymersattributes likehydrophobicity, molecular weight ($M_w$), and blockarrangement.Along these lines, copolymersstructure andcrystallinity of copolymers (hydrophobic/ hydrophilic segments) can be manipulated to form tailored platforms.

mPEG-PCL and PCL-mPEG-PCL PMs bearing the hydrophobic nutraceutical, ORZ, were formulated, owing to the self-assembling capability of the DB and TB copolymers usingthin film hydration technique, in order to obtain a well determined nanostructure as stated in our previous works(Elmowafy et al., 2019). Indeed, the inter-attraction between the hydrophilic PEG segment and water could be at the base of good dissolution and dispersability of hydrophobic drugs like ORZ in water(Hu et al., 2003). The DB and TB copolymers used in the preparation of ORZ micelle-coreoffer different molecular weights of 4 and 5kDa respectively. The impact of polymer structure (number of blocks of PEGylated PCL)andpolymer to drug ratio on physicochemical features of micelles was investigated.

The composition and physical parameters of the prepared micelle-core are depicted in Table 1.The selected anionic micelles were coated with positively charged CSby electrostatic interactions and the effect of CS coating was investigated as well.Inclusion of positive charge has been generally considered beneficial in improving oral absorption(Daeihamed et al., 2017). The composition and thecharacteristicphysical properties of chito-micelles are outlined in Table 3.

### 3.1. Colloidal parameters of the Micelle-core formulations

The impact of nanosized particles on oral transmucosal permeation and absorptionhas been well documented(Daeihamed et al., 2017).Dynamic light scattering revealed that the average diameter of the micelle-core was maintained below 200 nm, ranging from 97.9 to 117.8 nm.Obviously, the maximum value of PS was obtained upon using TB copolymer of $M_w$ 5kDa and polymer to ORZ ratio of 5:1 "PS value of M3 =117.8 nm" (table (1)).

The results also exhibited that increasing number of blocks of PEGylated PCL and hence copolymer molecular weight and lengthyielded extremely significant increase in micelles size at 5:1polymer to ORZ ratio only ($p<0.0001$). As the self-assembly of amphiphilic block copolymers in aqueous solutions involves mostly hydrophobic interactions(Yan and Xie, 2013),

these interaction might be potentiated by increasing the hydrophobicity and hence led to large micelle size (Alibolandi et al., 2015). Our results are in accordance with previouslyreported works. However, at higher polymer to ORZ ratio (10:1), MS differences were not remarkable exhibitingsimilar smaller micelle-core sizes for both BD and TD copolymers (98.88 *vs.* 97.9; insignificant, p=0.8872).This might infer the attainment of the well-knit polymeric micelles structure at this ratio (10:1). The steric hindrance conferred by increasing the hydrophilic PEG segment might lead to lower secondary agglomeration of the prepared micelles. This was consistent with As Aboud et al. who reported that increasing poloxamer F127 concentration was accompanied by a significant decrease in PS owing to the increase in hydrophilic ethylene oxide groups and hence steric hindrance preventing aggregate formation(Aboud et al., 2020).

The prepared nanovehicles were revealed to be stable with respect to narrow size distribution and negative surface charge.It can be noted that the PDI values were acceptable (0.219- 0.381) indicating particles homogeneity and monodispersion. As for surface charge, the micelle-corepossessed negative chargewith ZP values fitted between -12.6±2.1 and -29.2±2.54 mV. This could be attributed to theionized carboxyl groups of PCL hydrophobic segment. Compared with TB based micelle-core, lower ZP valueswere obtained for DB basedmicelle-corethatcould be assigned to the shielding effect of the neutral PEG shell. Previous studies revealed that increasing the polymer molecular weight was associated with increasing the negativity of ZP values, which may be attributed to the increase of hydrophobicity of the polymer as a function of the molecular weight. Unlike its impact on PS, shifting from 5:1 to 10:1 polymer to ORZ ratio displayed statistically invarient surface charge ($p > 0.05$).

### 3.2. ORZ entrapment efficiency and loading in the Micelle-core formulation

The percent of ORZ entrapped within micelle-core was found to be in the range of 67.28 to 93.87% while the DL% ranged between 7.93 and 17%.Higher values of EE% and DL% were observed in TB micelle-core rather than DB ones.Both EE% and DL% seemed to be strongly correlated with the number of blocks and polymer to ORZ ratio ($p<0.05$).

Concerning EE%, the feed ratio of the polymer to drug altered the amount of entrapped drug inmicellar system asthe EE%of micelle-core was increasedby 9-12% along with the increase in the polymer to ORZ ratio from 5:1 to 10:1. Higher impact on EE% was noticed for copolymer type, exhibiting 15-18% increase in EE% when shifting for DB copolymer to TB counterpart.

The highest EE% value was obtained in M4 prepared using TB copolymer at 10:1 polymer to ORZ ratio. This could be attributed to the greater amount of copolymer available to accommodate drug duringmicelles' formation. Additionally, the higher hydrophobicity of TB copolymer could intensify the hydrophobic interactions between ORZ and hydrophobic chains of the copolymer resulting in reduced drug distribution to the aqueous phase(Feng et al., 2012). These findings could reflect the competence of TB copolymer based micelle-core to retain shell integrity affecting ORZ entrapment.

As for the DL% , its trend was noticeably different from that of EE%. Likewise its impact on EE%, utilizing TB copolymer was demonstrated to favor significantly DL% optimization relative to BD copolymer. Most notably, varying D/P ratio exhibited a significant antagonistic effect on DL% ($p<0.05$). As depicted, increasing polymer molecular weightresulted in a significant reduction in %EE. Increasing the polymer amount led to a concomitant increase in the total mass of micelle-core. As a result, the DL% values significantly decreased when shifting from 5:1 to 10:1 polymer to ORZ ratio ($p < 0.05$).MaximumDL% was achieved whenTB copolymer was used at 5:1 polymer to ORZ ratio (DL% value =17.00%).

It is worth mentioning that there was a positive correlation between PS and DL% as when the drug incorporated inside the micelle-core, its volume increased accordingly(Feng et al., 2012). Similar findings were observed when using **triblock (PCL-PEG-PCL) and pentablock (PLA-PCL-PEG-PCL-PLA)** in loading auraptene(Jalilzadeh et al., 2020).

Based on the previous findings, M1 and M3 formulae prepared using 5:1 polymer to ORZ ratio and exhibited the highest DL% values (13.45 % and 17% respectively) were selected for CS coating andfurther investigations.

### 3.3. Impact of chitosan coating on colloidal parameters of the micelle-core

The formed coating layer on the micelle-core surface was found to impact the colloidal parameters of the micelle-core. Compared to the original micelle-core size, whatever the copolymer structure, the selected CS coated micelle-core (chito-micelles) exhibited significantly large diameters ($p < 0.05$).For both DB and TB copolymers, when the CS concentration increased from 0.25 to 0.5%, the MSincreased accordingly ($p < 0.05$). Besides, the chito-micelles size increased significantly upon further increase in CS concentration from 0.5 to 1%, yet, yielding PS> 200 nm. The highest CS concentration used (1%) was accompanied with a

significant increase in chito-micelles size (respective values for DB and TB chito-micelles were 411±12.75 and 480±10.68; $p < 0.05$) as profiled in Table 3. The increased thickness accompanied with increasing CS concentration led to particles sizes enlargement.

Similarly, PDI showed strong dependenceon CS coating referring to heterodisperse colloidal systems. For example,upon using the highest CS concentration (1%) in both DB and TB copolymers, the resultant formulations were found to be more polydisperse (respective values of 0.61 and 0.927). The concomitant increase in PS and PDI with the increase in CS concentration was noted in previous investigations(Pandit et al., 2017).

Meanwhile, the total nanoplatformcharge reversed from negative charge (for micelle-core) to positive charge (for micelle-core/CS shell nanoplatforms), pinpointing the deposition of CS layer on the surface of micelle-core and hence the infallible coating.This came in line with previous literature for CS coated solid lipid nanoparticles(Kamel et al., 2017)and CS coated nano-liposomes(Nguyen et al., 2014). The magnitude of the zeta potential values was noticeably increased with the increment in CS concentration. Importantly, the high values of absolute zeta potential indicated high in vitro stability.

It is worth mentioning that using CS concentrations up to 0.5% yielded coated nanoplatforms with size less than 200 nm that are optimal for the felicitousdiffusion of nanoparticles through intestinal mucus layer(Yun et al., 2013).

### 3.4. Morphological examination

Fig.1 shows a representative TEM image of the selected micelle-core (M3) and the corresponding chito-micelles (C-$M3_{(0.5)}$). As revealed, the preparednanovehicles were nearly spherical with a size similar to particle size measurement using the dynamic light scattering technique. The particle surface wasvery smooth and no drug crystal was visible. CS coating was confirmed in the chito-micelles.Sizes are in agreement with the DLS analysis.

### *3.5. In-vitro*release study and release kinetics

In order to investigate the effect of number of PCL copolymer blocks on one side and CS coating on the other side on ORZ release behaviorfrom the prepared nanoplatforms, the *in-vitro*release study of ORZ from selected micelle-core formulae (M1 and M3) and the corresponding chito-micelles (C-$M1_{(0.5)}$ and C-$M13_{(0.5)}$)was performed using ORZ ethanolic solution as a control, as

shown in Fig. 2.ORZ solution was completely released within 8 h (data not shown) while all selected formulae exhibited sustained release properties that seemed to be well-linked to the molecular structural features of micelles and their further coating step.

For all the tested micelle-core formulae and chito-micelles, the accumulated release at 24 h exhibited two-stage release profile with an initial burst discharge in the first 2 h followed by a slower drug release for 24 h. The initial burst effect is correlated with the easily desorbed corona-entrapped drug while the slower drug release was attributed to the entrapped drug diffusion from the micelle-core. The initial burst release of ORZ in TB co-polymer based micelle-core (M3) was significantly lower than that in BD based one (M1).This two-phase release profile of the polymeric micelles came in line with previous literature(Feng et al., 2012; Gong et al., 2010).

As a consequence of CS coating, a significantly lower burst release was detected for Chito-micelles than that of the corresponding micelle-cores. The reduced burst discharge of the CS coated nanocarriers was demonstrated previously(Dasineh et al., 2021; Lu et al., 2019).Besides, after the initial rapid release, chito-micelles resulted in more sustained release. The cumulative release of ORZ from C-M1$_{(0.5)\ and}$ C-M13$_{(0.5)}$ was 53.9%, and 46.86%, after 24 h, respectively. The slow diffusion of ORZ from the preparednanosystems ensured the maintenance of constant ORZ concentration for a relatively long period of time. These findingswere in agreement with Nguyen et al. who reported the concentration-dependent retarding impact of CS coating on the Berberinehydrochloride release fromCS coated nano-liposomes(Nguyen et al., 2014).

ORZ release from selected uncoated and coated micellesshowed a good fit to the Higuchi model with the highest linearity ($r^2$= 0.923-0.947). Similarly, fitting to Peppas model exhibited acceptable linearity ($r^2$= 0.90-0.961) with values of around 0.20 (Fickian), indicating diffusion mediated drug release.

### 3.6. DSC

DSC study was performed to assess the physical stability of the nanoplatforms and encapsulation of ORZ inside them. The DSC curves obtained are shown in Fig. 3.ORZthermogram displayed endothermic melting peaks at60 °C, 99 °C&160 °C followed by exothermic peak at 175°C indicating drug decomposition at higher temperature.This thermal behavior proved the crystalline nature of the drug. As for thermograms of DB & TB copolymers, their DSC thermograms showed endothermic melting peaks at 60 & 140 °C for DB & 60 &100 °C for TB

as shown in Fig.3 . Upon investigating the thermograms of uncoated and CS coated DB and TB micelles, it was obvious that ORZ melting peaks disappearedupon encapsulation inside both CS coated and uncoated micelles indicating that ORZ was present within the micelles in an amorphous state proving its dissolution inside the matrix(Ruktanonchai et al., 2009).

### 3.7. FT-IR

FTIR was employed to disclose the possible interaction between ORZ and the polymeric micelles and prove the coating of the micelles with CS as shown in Fig.4**.** Ingenerated spectrum for ORZ, the different groups were represented by the following peaks: C-Hstretching of alkanes at 2954 $cm^{-1}$ of alkanes, C=C stretching of aromatic hydrocarbons at 1602/cm, intermolecular H bonded OH stretching of alcohol at 3298.68/cm and C=O stretching enolic groups of ester at 1689.34/cm of ester(Rawal et al., 2018).The DB copolymer showed characteristic high-intensity signals at 1726.64 $cm^{-1}$ for C=O vibrations,indicating the crystalline nature of the micelle core(Elmowafy et al., 2019),and weak bands at 3448.17 cm−1 for OH stretching vibrations.Higher intensity signals were more evident at 1726.64 in case of TB copolymer indicating higher crystallinity arising from the $2^{nd}$ PCL moiety.

In the spectrum of CS coated DB & TB micelles, the characteristic peak located at 3447 $cm^{-1}$ represented intermolecular hydrogen bonding and stretching vibration of –NH2 as well as –OH groups of CS.Another typical peak for CS, is the peak at 2900 $cm^{-1}$which representedthestretching vibration of C–H from alkyl groups, whereas peaks at around 1657 cm−1 (C=O stretching of amide I) and 1320 cm−1 (C−N stretching of amide III), respectively confirmed the presence of residual N-acetyl groups.Moreover, the presence of bands at 1428 and 1360 cm−1– proved the CH2 bending besides –CH3 symmetrical deformations respectively,while that at 1158 cm−1 could be attributed to asymmetric stretching of the C–O–C bridge. Besides, the bands at 1066 and 1029 cm−1 were related to C–O stretching.

However, in the spectrum of ORZ-DB copolymer micelles (M2), ORZ-TB copolymer micelles and CS coated micelles, noticeable weakening of the characteristic peaks of C-O and S-O stretching of ORZ as well as characteristic peaks of the different copolymers in addition to CS were observed. Such findings indicated the incorporation and amorphization of ORZ inside the different micelles.

### 3.8. Stability studies

Colloidal stability is a major concern with clinical oral administration of nanovehicles. In this regard, the effect of short term storage on the selected chitomicelles was monitored for four weeks at 4°C. As observed in Table 4, negligible variations in PS were recognized overfour weeks compared to the initial results (0 day) ($p>0.05$). However, a slight increase in PS, yet non-significant, was revealed at the end of storage period "28 days" ($p>0.05$).

It is worthy to note that values of PDI (0.424-0.485) and ZP (33.2- 37.8) exhibited no significant changes over four weeks ($p>0.05$). Referring to literature, CS coated nanoplatforms exhibited excellent stability(Quagliariello et al., 2018)**.**

Furthermore, to mimic thein vivo physiological intestinal conditions, *in vitro* stability study of the selected micelles in SIF was conducted at 37°C. The PS and PDI of micellar dispersions remained nearly unchanged after 6 h incubation ($p>0.05$). These results confirmed the stability of the micelles in the intestinal environment. This was consistent with previous findings(Ji et al., 2018).

Considering the above mentioned findings, TB based nanoplatform (C-$M3_{(0.5)}$) was a promising nanoplatformfor ORZ with respect with high drug loading and prolonged release and were subjected to subsequent in vitro and in vivo investigations. For comparative purposes, to elucidate the influence of CS coating, the uncoated micelles-core (M3) were also examined.

### 3.9. Mucoadhesion

The in vitro mucoadhesiveness of the selected chito-micelles were demonstrated via the measurement of their ζ-potential values. Following the incubation of chito-micelles with mucin, a remarkable 3.72 fold reduction in the magnitude of the zeta potential value was attained (37.4±0.781 versus 10.03±0.36). This behavior indicated the paramount ionic interaction between the positive charge of CS coated micelles by negatively charged mucin groups(Elmowafy and Soliman, 2019) and hence considerable mucoadhesivity. This was consistent with previously published reports(Hejjaji et al., 2018; Silva et al., 2017). This wasnot the case in the micelle-core-mucinmixture that exhibited negative zeta potential value of -10.5±5.23.Similarly, the PS of chito-micelles was significantly increased in the presence of mucin( 318.9±2.43 nm) ($p <0.05$).

### *3.10. In vitro* anti-oxidant potential

ORZ has been documented to possess antioxidant activity. The results of DPPH assay depicted that theformulation process of micelle-core and chito-micelles did not interfere with ORZ antioxidant capacity in vitro. While both micelle-core and chito-micelles exhibited free radical scavenging ability,the chito-micellespossessed greater antioxidant activity (**92.63** ± 1.59%) as compared to micelle-core (**78.56** ± 2.62%). Interestingly, chito-micelles showed similar DPPH scavenging to the standard antioxidant; ascorbic acid (**98.76** ± 0.62%).Greater antioxidant activity of CS coated nanosystemsas compared to its uncoated ones was demonstrated earlier(Quagliariello et al., 2018).

### *3.11. In vitro* cytocompatibility

The available literature data point to the biocompatibility of PCL copolymers on different cell lines(Gong et al., 2013; Łukasiewicz et al., 2021).Safe effect on cell lines was reported for pegylatednanopartilcles as well as CS based nanoparticles.Specifically, no cytotoxicity on caco-2 cells (model of intestinal epithelium) have been revealed for CS nanoparticles(Liu et al., 2013).This was stemmed from the fact that they were formed bio-acceptable components.

MTT assay was employed to investigate the proliferation ofVERO cells after 24 h incubation of different concentrations of unformulated ORZ,ORZ micelle-core and the corresponding chito-micelles. The highest cytocompatable effects were observed in chito-micellescompared to micelle-core and free ORZobtained by MTT assay, As evident in Fig.5,unformulated ORZ treatment for 24 h dramatically decreased vero cells viability in a concentration dependent manner reaching only 19.45% cell viability at 250 µg/mL.On the other hand, the viability of vero cells treated with micelle-core and chito-micelles at the highest concentration (250 µg/mL) was about 45% and 50% higher, respectively versus ORZ-treated cells. Furthermore, statistical difference in cell viability was noticed between formulated ORZ and unformulated ORZ at all the tested concentrations ($p < 0.05$). More importantly, chito-micelleswere revealed to have better cytocompatability properties than did micelle-core. Worthy to note thatchito-micelles showed slightly 70.82% cell viability at the highest concentration (250 µg/mL), the minimum threshold for cytotoxicity. IC50% of the micelle-core and its corresponding chito-micelles was found to be 383.1 and415.8µg/mL respectively, being 4.41 fold and 4.79 fold increase in cell viability when compared to free ORZ which showed moderate cytotoxicity ($IC_{50}$= 86.7 µg/mL). This indicates the positive effect of CS on improving the safety

of chito-micelles. Thus, theselected formulawas tolerable and would not cause renal cytotoxicity (IC50>

### *3.12. In vivo* pharmacodynamic study

Indeed, the bioavailability of a drug after administration and its pharmacodynamics are strongly correlated. Substantial drug bioavailability could be reflected by its intensified pharmacological effect. In line, the nephroprotective effect of ORZ and its uncoated and coated micelles were investigated in glycerol-induced AKI model, strongly reflectingrhabdomyolysis(Adedapo et al., 2021).IM injection of hypertonic concentration of glycerol was reported to bring about myolysis, hemolysis and tubular nephrotoxic effects induced by renal exposuretoheme proteins and their degradation products(BALIGA et al., 1999; de Jesus Soares et al., 2007).Additionally, glycerol-induced AKI was accompanied by myoglobin toxicity, oxidative damage, inflammation andapoptois(Adedapo et al., 2021; Wu et al., 2017). The protective effect of ORZon cardio-renal syndrome, induced by administration of high-fat-sucrose diet and cisplatin injection, has beenconfirmed with respect to improvement of kidney function parametersand glomerular filteration rate(Al-Okbi et al., 2019).

A significant boost in serum urea and creatinine levels of the toxicant AKI group was revealed, an attestation to the occurrence of glycerol-induced renal damage, **Fig.6**. This came in line with previous literature (Hashish et al., 2020). The disrupted serum urea and creatinine levels in AKI group were significantly ameliorated by the pretreatment of rats withORZ either suspension, micelle-core or chito-micelles ($p < 0.05$).ORZ suspension and micelle-core descended the kidney function parameters by approximately 1.35 -1.65 folds for urea and 1.36-2 folds for creatinine respectively relative to AKI group ($p< 0.05$).Yet, the greatest impact was noticed with chito-micelles. Chito-micelles showed nearly two- and four-fold decline in serum urea and creatinine levels respectively compared to AKI group ($p< 0.05$), approaching that of the normal control group ($p> 0.05$).

The superior biological performance of chito-micelles can be credited to several factors. First, the mucoadhesive nature and paracellular permeability enhancing effect of the outer CS layer helps increasing intestinal absorption of ORZ(Liu et al., 2013). Second, CS itself has renal protection and targeting properties as a result of its increased renal concentration due to its preferential distribution to the kidney(Chou et al., 2015). In a previous study conducted by Liu et al. that CS nanoparticles(mean diameter of 215.34 nm, zeta potential of 19.26 mV)distributed

mainly in liver, kidney and heart and this was attributed to its infiltration into the mucus layer and long residence in blood circulation(Liu et al., 2013). Third, the nano size and sustainedrelease properties of the formed chito-micelles. The beneficial effects of ORZ in reversing renal dysfunctioncould be related to its anti-inflammatory, cytoprotective, and antioxidant actions in the kidney. To elucidate these benefits, the renal morphological alterations andunderlying molecular mechanismwere thoroughly investigated.

### 3.13. Chitosan coated and uncoated ORZ attenuated histopathological alteration of glycerol induced acute kidney injury

Histological examination of H&E stained kidney sections **(Fig. 7)** showed no histopathological changes in the control group. However, glycerol induced acute kidney injury showing abundant necrotic and hyperesenophilic tubular segments areas losing its luminal border integrity as well as cystic dilatation of some tubules and higher records of intraluminal desquamated epithelial cells and casts. Moreover, congested interstitial blood vessels were also shown. Treatment with free ORZ showed diffuse moderate tubular degenerative changes with many figures of vacuolar degeneration of various tubular segments associated with necrotic cells, mild focal records of intraluminal cellular casts and mild congested interstitial blood vessels. On the other hand, uncoated micelle group showed protective effects with moderate records of tubular vacuolar degenerative changes associated with few focal records of tubular necrosis. Chitosan coated ORZ group demonstrated superior protective effects through mild focal records of tubular degenerative changes and nuclear pyknosis. Besides, abundant records of intact nephronal segments were shown with intact vasculatures of the renal corpuscles **(Fig. 7)**. Scoring of the kidney tissues showed marked congestion in the blood vessels, associated with severe tubular necrosis and abundance of luminal casts with moderate cystic dilatation in glycerol induced acute kidney injury as compared to the control group. In alignment, treatment with free ORZ didn't show significant improvement in renal damage scoring. However, moderate improvement was observed in uncoated micelle group, while, significant protection was detected in Chitosan coated γ ORZ group showing mild tubular necrosis and mild luminal casts **(Fig. 7)**.

### 3.14. Sirtuin-1 signaling pathway and associated machineries

#### 3.14.1. Chitosan coated and uncoated ORZ increased sirtuin-1 levels in glycerol induced acute kidney injury

A significant decrease was found in Sirtuin-1 levels in AKI as compared to the control group. Otherwise, treating with ORZ uncoated or CS coated micelles significantly increased sirtuin-1 levels by 16.9% and 11.2% as compared to AKI group (**Fig. 8**).

#### 3.14.2. Chitosan coated and uncoated ORZ increased the antioxidant states in glycerol induced acute kidney injury

Antioxidant state was significantly suppressed in acute kidney injury evidenced by significant decrease in MnSOD, UCP2 and PGC-1α by 51.2%, 76.2% and 67% respectively. However, all free ORZ and ORZ incorporated in uncoated and coated micelles significantly stimulated the antioxidant state as shown in **Fig. 9.**

#### 3.14.3. Chitosan coated and uncoated ORZ activated autophagy in glycerol induced acute kidney injury

Autophagy was significantly abrogated in AKI group as shown in **Fig. 10** with remarkable decrease in expression of ATG 5,7, 12 and in ULK-1. On the other side, ORZuncoated and CS coated micelles significantly increased the expression of autophagy regulated genes.

#### 3.14.4. Chitosan coated and uncoated ORZ abrogated inflammation in glycerol induced AKI

Acute kidney injury is associated with increased inflammation which was clearly shown in our results with significant increase in IL-6 by 96.7% and in IL-1β by 115.5% and in TGF-β by 56.9% as compared to the control group. Reversibly, Chitosan coated and uncoated ORZ micelles significantly resolved this inflammatory changes as shown in **Fig. 11.**

#### 3.14.5.Chitosan coated and uncoated ORZ diminishedapoptotic changes in glycerol induced acute kidney injury

The expression of apoptotic genes p53, PUMA and Bax/Bcl2 ration were significantly induced in AKI as shown in **fig. 12.** Nevertheless, Chitosan coated and uncoated ORZ micelles significantly diminished this apoptotic state.

To sum up, free ORZ failed to protect against glycerol induced AKI with moderate necrotic and degenerative changes. However, Chitosan coated and uncoated ORZ micelles significantly restored renal antioxidant states through the upregulationof MnSOD, UCP2 and PCG-1α genes. This was associated with autophagy activation via increasing the expression of ATG 5, ATG 7, ATG 12 and ULK-1. Furthermore, this was accompanied by inhibiting inflammation through decreasing renal levels of IL-6, IL-1β and TGF-β which leads to diminishing apoptosis through decreased renal expression of p53, PUMA and BAX/BcL2 ratio. All these effects are reported to be through increasing renal sirtuin-1 levels.

## 4. Conclusion

Chitosan (CS) coated and uncoated copolymer micelles of the phytochemical drug, ORZ were successfully prepared. The prepared micelles showed favorable nanosize, zetapotenial and PDI. Additionally, the prepared micelles exhibited high DL% & EE% forORZ in addition to sustained drug release pattern. Both micelles showed cytocompatibility on Vero® cells of the kidney with the chito-micelles showing higher safety than uncoated. The modification and coating of micellar surface with chitosan was proved by the size increase and charge reversal upon coating with chitosan, in addition to the DSC and FTIR studies. The nephroprotective effect of the prepared micelles against glycerol induced acute renal impairment in rats was proved through measurement of nephrotoxic indices, serum urea &creatininelevels in rats serum, histopathological examination, biochemical measurement of sirtulin-1 levels, antioxidant, autophagy and apoptotic genes in different experimental groups. Both chitosan coated and uncoated micelles exhibited better nephroprotective potential compared to free ORZ suspension. Additionally, CS coated micelles were more effective on restoring normal kidney parameters to than uncoated ones. Hence, these newly developed nanoformulations of the phytochemical drug ORZ are considered promising platforms for protection against acute kidney impairment.

## References

Aboud, H.M., Mahmoud, M.O., Abdeltawab Mohammed, M., Shafiq Awad, M., Sabry, D., 2020. Preparation and appraisal of self-assembled valsartan-loaded amalgamated Pluronic F127/Tween 80 polymeric micelles: boosted cardioprotection via regulation of Mhrt/Nrf2 and Trx1 pathways in cisplatin-induced cardiotoxicity. Journal of drug targeting 28, 282-299.

694 Adedapo, A.A., Osaretin, E.R., Falayi, O.O., Oyagbemi, A.A., Ogunpolu, B.S., Omobowale,
695 T.O., Oguntibeju, O.O., Yakubu, M.A., 2021. Ramipril blunts glycerol-induced acute renal
696 failure in rats through its antiapoptosis, anti-inflammatory, antioxidant, and renin-inhibiting
697 properties. Journal of Basic and Clinical Physiology and Pharmacology 32, 225-235.
698 Ahmad, Z., Shah, A., Siddiq, M., Kraatz, H.-B., 2014. Polymeric micelles as drug delivery
699 vehicles. Rsc Advances 4, 17028-17038.
700 Al-Okbi, S.Y., Mohamed, D.A., Hamed, T.E., Al-Siedy, E.S., 2019. Rice bran as source of
701 nutraceuticals for management of cardiovascular diseases, cardio-renal syndrome and hepatic
702 cancer. Journal of Herbmed Pharmacology 9, 68-74.
703 Aldalaen, S., Nasr, M., El-Gogary, R.I., 2020. Angiogenesis and collagen promoting
704 nutraceutical-loaded nanovesicles for wound healing. Journal of Drug Delivery Science and
705 Technology 56, 101548.
706 Alibolandi, M., Ramezani, M., Abnous, K., Sadeghi, F., Hadizadeh, F., 2015. Comparative
707 evaluation of polymersome versus micelle structures as vehicles for the controlled release of
708 drugs. Journal of Nanoparticle Research 17, 1-16.
709 Aslam, S., Jahan, N., Rehman, K.-u., Asi, M.R., 2020. Development of sodium lauryl sulphate
710 stabilized nanosuspension of Coriandrum sativum to enhance its oral bioavailability. Journal of
711 Drug Delivery Science and Technology 60, 101957.
712 Azab, A.E., Albasha, M.O., Elsayed, A.S.I., 2017. Prevention of nephropathy by some natural
713 sources of antioxidants. Yangtze Medicine 1, 235.
714 BALIGA, R., UEDA, N., WALKER, P.D., SHAH, S.V., 1999. Oxidant mechanisms in toxic
715 acute renal failure. Drug metabolism reviews 31, 971-997.
716 Cheng, W., Zeng, X., Chen, H., Li, Z., Zeng, W., Mei, L., Zhao, Y., 2019. Versatile
717 polydopamine platforms: synthesis and promising applications for surface modification and
718 advanced nanomedicine. Acs Nano 13, 8537-8565.
719 Chou, C.-K., Li, Y.-C., Chen, S.-M., Shih, Y.-M., Lee, J.-A., 2015. Chitosan prevents
720 gentamicin-induced nephrotoxicity via a carbonyl stress-dependent pathway. BioMed research
721 international 2015.
722 Daeihamed, M., Haeri, A., Ostad, S.N., Akhlaghi, M.F., Dadashzadeh, S., 2017. Doxorubicin-
723 loaded liposomes: enhancing the oral bioavailability by modulation of physicochemical
724 characteristics. Nanomedicine 12, 1187-1202.

Dasineh, S., Akbarian, M., Ebrahimi, H.A., Behbudi, G., 2021. Tacrolimus-loaded chitosan-coated nanostructured lipid carriers: preparation, optimization and physicochemical characterization. Applied Nanoscience 11, 1169-1181.

de C Coelho Junior, É., Maciel, P.P., de AF Muniz, I., Silva, H.Y., de Sousa, S.A., Valença, A.M., Dias, R.T., Batista, A.U., Figueiredo, L.R., de Medeiros, E.S., 2021. Poloxamer 407/chitosan micelles can improve α-Tocopherol effect on oral keratinocytes proliferation. Journal of Materials Research 36, 1447-1455.

de Jesus Soares, T., Volpini, R.A., Francescato, H.D., Costa, R.S., da Silva, C.G., Coimbra, T.M., 2007. Effects of resveratrol on glycerol-induced renal injury. Life sciences 81, 647-656.

El-Gogary, R.I., Nasr, M., Rahsed, L.A., Hamzawy, M.A., 2022. Ferulic acid nanocapsules as a promising treatment modality for colorectal cancer: Preparation and in vitro/in vivo appraisal. Life Sciences 298, 120500.

Elmowafy, E., El-Derany, M.O., Biondo, F., Tiboni, M., Casettari, L., Soliman, M.E., 2020. Quercetin loaded monolaurate sugar esters-based niosomes: Sustained release and mutual antioxidant—hepatoprotective interplay. Pharmaceutics 12, 143.

Elmowafy, E., Gad, H., Biondo, F., Casettari, L., Soliman, M.E., 2019. Exploring optimized methoxy poly (ethylene glycol)-block-poly (ε-caprolactone) crystalline cored micelles in anti-glaucoma pharmacotherapy. International journal of pharmaceutics 566, 573-584.

Elmowafy, E., Soliman, M.E., 2019. Losartan-chitosan/dextran sulfate microplex as a carrier to lung therapeutics: dry powder inhalation, aerodynamic profile and pulmonary tolerability. International journal of biological macromolecules 136, 220-229.

Feng, R., Song, Z., Zhai, G., 2012. Preparation and in vivo pharmacokinetics of curcumin-loaded PCL-PEG-PCL triblock copolymeric nanoparticles. International journal of nanomedicine 7, 4089.

Gad, H.A., Mansour, M., Abbas, H., Malatani, R.T., Khattab, M.A., Elmowafy, E., 2022. “Plurol will not miss the boat”: A new manifesto of galantamine conveyance. Journal of Drug Delivery Science and Technology, 103516.

Ghaderi, S., Ghanbarzadeh, S., Mohammadhassani, Z., Hamishehkar, H., 2014. Formulation of gammaoryzanol-loaded nanoparticles for potential application in fortifying food products. Advanced pharmaceutical bulletin 4, 549.

Gong, C., Deng, S., Wu, Q., Xiang, M., Wei, X., Li, L., Gao, X., Wang, B., Sun, L., Chen, Y., 2013. Improving antiangiogenesis and anti-tumor activity of curcumin by biodegradable polymeric micelles. Biomaterials 34, 1413-1432.

Gong, C., Wei, X., Wang, X., Wang, Y., Guo, G., Mao, Y., Luo, F., Qian, Z., 2010. Biodegradable self-assembled PEG–PCL–PEG micelles for hydrophobic honokiol delivery: I. Preparation and characterization. Nanotechnology 21, 215103.

Hashish, E., Elgaml, S., El-Fattah, A., Shalaby, S., Abdelaziz, S., 2020. β-Amyrin supplementation ameliorates the toxic effect of glycerol in the kidney of rat model. Human & experimental toxicology 39, 930-937.

Hejjaji, E.M., Smith, A.M., Morris, G.A., 2018. Evaluation of the mucoadhesive properties of chitosan nanoparticles prepared using different chitosan to tripolyphosphate (CS: TPP) ratios. International journal of biological macromolecules 120, 1610-1617.

Hou, Y., Wang, H., Zhang, F., Sun, F., Xin, M., Li, M., Li, J., Wu, X., 2019. Novel self-nanomicellizing solid dispersion based on rebaudioside A: a potential nanoplatform for oral delivery of curcumin. International journal of nanomedicine 14, 557.

Hu, Y., Jiang, X., Ding, Y., Zhang, L., Yang, C., Zhang, J., Chen, J., Yang, Y., 2003. Preparation and drug release behaviors of nimodipine-loaded poly (caprolactone)–poly (ethylene oxide)–polylactide amphiphilic copolymer nanoparticles. Biomaterials 24, 2395-2404.

Jalilzadeh, N., Samadi, N., Salehi, R., Dehghan, G., Iranshahi, M., Dadpour, M.R., Hamishehkar, H., 2020. Novel nano-vehicle for delivery and efficiency of anticancer auraptene against colon cancer cells. Scientific reports 10, 1-19.

Ji, S., Lin, X., Yu, E., Dian, C., Yan, X., Li, L., Zhang, M., Zhao, W., Dian, L., 2018. Curcumin-loaded mixed micelles: Preparation, characterization, and in vitro antitumor activity. Journal of Nanotechnology 2018.

Kamel, K.M., Khalil, I.A., Rateb, M.E., Elgendy, H., Elhawary, S., 2017. Chitosan-coated cinnamon/oregano-loaded solid lipid nanoparticles to augment 5-fluorouracil cytotoxicity for colorectal cancer: extract standardization, nanoparticle optimization, and cytotoxicity evaluation. Journal of agricultural and food chemistry 65, 7966-7981.

Kengkittipat, W., Kaewmalun, S., Khongkow, M., Iempridee, T., Jantimaporn, A., Bunwatcharaphansakun, P., Yostawonkul, J., Yata, T., Phoolcharoen, W., Namdee, K., 2021.

785 Improvement of the multi-performance biocharacteristics of cordycepin using BiloNiosome-
786 core/chitosan-shell hybrid nanocarriers. Colloids and Surfaces B: Biointerfaces 197, 111369.
787 Kumar, R., Sirvi, A., Kaur, S., Samal, S.K., Roy, S., Sangamwar, A.T., 2020. Polymeric micelles
788 based on amphiphilic oleic acid modified carboxymethyl chitosan for oral drug delivery of bcs
789 class iv compound: Intestinal permeability and pharmacokinetic evaluation. European Journal of
790 Pharmaceutical Sciences 153, 105466.
791 Lamie, C., Elmowafy, E., Attia, D.A., Elmazar, M.M., Mortada, N.D., 2022. Diversifying the
792 skin cancer-fighting worthwhile frontiers: How relevant are the itraconazole/ascorbyl palmitate
793 nanovectors? Nanomedicine: Nanotechnology, Biology and Medicine 43, 102561.
794 Liu, Y., Kong, M., Feng, C., Yang, K.K., Li, Y., Su, J., Cheng, X.J., Park, H.J., Chen, X.G.,
795 2013. Biocompatibility, cellular uptake and biodistribution of the polymeric amphiphilic
796 nanoparticles as oral drug carriers. Colloids and Surfaces B: Biointerfaces 103, 345-353.
797 Lu, B., Lv, X., Le, Y., 2019. Chitosan-modified PLGA nanoparticles for control-released drug
798 delivery. Polymers 11, 304.
799 Łukasiewicz, S., Mikołajczyk, A., Błasiak, E., Fic, E., Dziedzicka-Wasylewska, M., 2021.
800 Polycaprolactone nanoparticles as promising candidates for nanocarriers in novel nanomedicines.
801 Pharmaceutics 13, 191.
802 Manosroi, A., Chutoprapat, R., Abe, M., Manosroi, W., Manosroi, J., 2012. Transdermal
803 absorption enhancement of rice bran bioactive compounds entrapped in niosomes. AAPS
804 PharmSciTech 13, 323-335.
805 Nguyen, T.X., Huang, L., Liu, L., Abdalla, A.M.E., Gauthier, M., Yang, G., 2014. Chitosan-
806 coated nano-liposomes for the oral delivery of berberine hydrochloride. Journal of Materials
807 Chemistry B 2, 7149-7159.
808 Pandit, J., Sultana, Y., Aqil, M., 2017. Chitosan-coated PLGA nanoparticles of bevacizumab as
809 novel drug delivery to target retina: optimization, characterization, and in vitro toxicity
810 evaluation. Artificial cells, nanomedicine, and biotechnology 45, 1397-1407.
811 Patra, A., Satpathy, S., Shenoy, A.K., Bush, J.A., Kazi, M., Hussain, M.D., 2018. Formulation
812 and evaluation of mixed polymeric micelles of quercetin for treatment of breast, ovarian, and
813 multidrug resistant cancers. International journal of nanomedicine 13, 2869.
814 Quagliariello, V., Vecchione, R., Coppola, C., Di Cicco, C., De Capua, A., Piscopo, G., Paciello,
815 R., Narciso, V., Formisano, C., Taglialatela-Scafati, O., 2018. Cardioprotective effects of

816 nanoemulsions loaded with anti-inflammatory nutraceuticals against doxorubicin-induced
817 cardiotoxicity. Nutrients 10, 1304.
818 Rawal, T., Mishra, N., Jha, A., Bhatt, A., Tyagi, R.K., Panchal, S., Butani, S., 2018. Chitosan
819 nanoparticles of gamma-oryzanol: Formulation, optimization, and in vivo evaluation of anti-
820 hyperlipidemic activity. Aaps Pharmscitech 19, 1894-1907.
821 Ruktanonchai, U., Sakulkhu, U., Bejrapha, P., Opanasopit, P., Bunyapraphatsara, N.,
822 Junyaprasert, V., Puttipipatkhachorn, S., 2009. Effect of lipid types on physicochemical
823 characteristics, stability and antioxidant activity of gamma-oryzanol-loaded lipid nanoparticles.
824 Journal of microencapsulation 26, 614-626.
825 Seetapan, N., Bejrapha, P., Srinuanchai, W., Ruktanonchai, U.R., 2010. Rheological and
826 morphological characterizations on physical stability of gamma-oryzanol-loaded solid lipid
827 nanoparticles (SLNs). Micron 41, 51-58.
828 Shalaby, K.S., Soliman, M.E., Bonacucina, G., Cespi, M., Palmieri, G.F., Sammour, O.A., El
829 Shamy, A.A., Illum, L., Casettari, L., 2016. Nanoparticles Based on Linear and Star-Shaped
830 Poly(Ethylene Glycol)-Poly(ε-Caprolactone) Copolymers for the Delivery of Antitubulin Drug.
831 Pharmaceutical Research 33, 2010-2024.
832 Shalaby, K.S., Soliman, M.E., Casettari, L., Bonacucina, G., Cespi, M., Palmieri, G.F.,
833 Sammour, O.A., El Shamy, A.A., 2014. Determination of factors controlling the particle size and
834 entrapment efficiency of noscapine in PEG/PLA nanoparticles using artificial neural networks.
835 International journal of nanomedicine 9, 4953.
836 Silva, M.M., Calado, R., Marto, J., Bettencourt, A., Almeida, A.J., Gonçalves, L., 2017. Chitosan
837 nanoparticles as a mucoadhesive drug delivery system for ocular administration. Marine drugs
838 15, 370.
839 Song, X., Pang, H., Cui, W., Zhang, J., Li, J., Jia, L., 2021. Renoprotective effects of enzyme-
840 hydrolyzed polysaccharides from Auricularia polytricha on adenine-induced chronic kidney
841 diseases in mice. Biomedicine & Pharmacotherapy 135, 111004.
842 Tentor, F.R., de Oliveira, J.H., Scariot, D.B., Lazarin-Bidoia, D., Bonafe, E.G., Nakamura, C.V.,
843 Venter, S.A., Monteiro, J.P., Muniz, E.C., Martins, A.F., 2017. Scaffolds based on
844 chitosan/pectin thermosensitive hydrogels containing gold nanoparticles. International journal of
845 biological macromolecules 102, 1186-1194.

Tiboni, M., Elmowafy, E., El-Derany, M.O., Benedetti, S., Campana, R., Verboni, M., Potenza, L., Palma, F., Citterio, B., Sisti, M., 2022. A combination of sugar esters and chitosan to promote in vivo wound care. International Journal of Pharmaceutics 616, 121508.

Viriyaroj, A., Ngawhirunpat, T., Sukma, M., Akkaramongkolporn, P., Ruktanonchai, U., Opanasopit, P., 2009. Physicochemical properties and antioxidant activity of gamma-oryzanol-loaded liposome formulations for topical use. Pharmaceutical development and technology 14, 665-671.

Wu, H., Huang, J., 2018. Drug-induced nephrotoxicity: pathogenic mechanisms, biomarkers and prevention strategies. Current drug metabolism 19, 559-567.

Wu, J., Pan, X., Fu, H., Zheng, Y., Dai, Y., Yin, Y., Chen, Q., Hao, Q., Bao, D., Hou, D., 2017. Effect of curcumin on glycerol-induced acute kidney injury in rats. Scientific reports 7, 1-11.

Yan, L.-T., Xie, X.-M., 2013. Computational modeling and simulation of nanoparticle self-assembly in polymeric systems: Structures, properties and external field effects. Progress in Polymer Science 38, 369-405.

Yang, K.-M., Chiang, P.-Y., 2019. Preparation and evaluation of release formulation of γ-oryzanol/algae oil self-emulsified with alginate beads. Marine Drugs 17, 156.

Yun, Y., Cho, Y.W., Park, K., 2013. Nanoparticles for oral delivery: targeted nanoparticles with peptidic ligands for oral protein delivery. Advanced drug delivery reviews 65, 822-832.

Zhang, Q., Polyakov, N.E., Chistyachenko, Y.S., Khvostov, M.V., Frolova, T.S., Tolstikova, T.G., Dushkin, A.V., Su, W., 2018. Preparation of curcumin self-micelle solid dispersion with enhanced bioavailability and cytotoxic activity by mechanochemistry. Drug Delivery 25, 198-209.

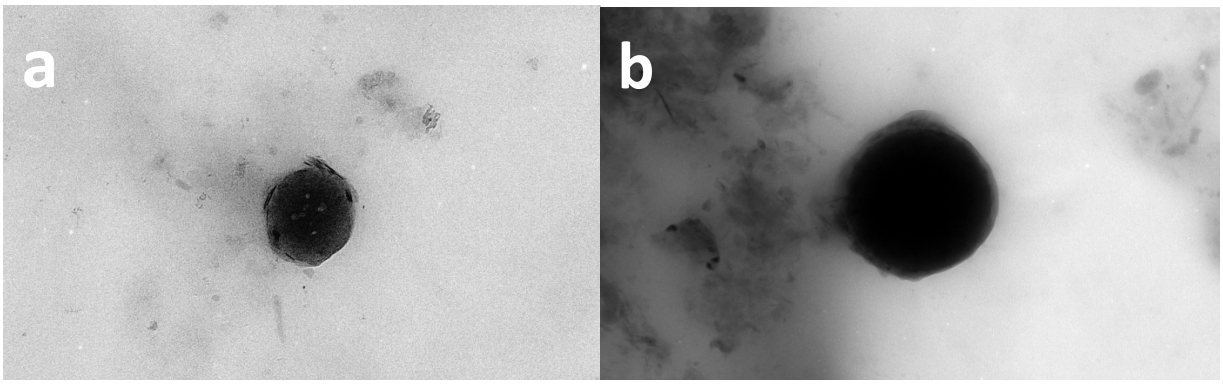


**Fig. 1: Transmission electron microscope (TEM) images of : a) uncoated micelles (M3) and b) chitosan coated micelles ( C-M3$_{(0.5)}$) visualized under a voltage of 200 kV**

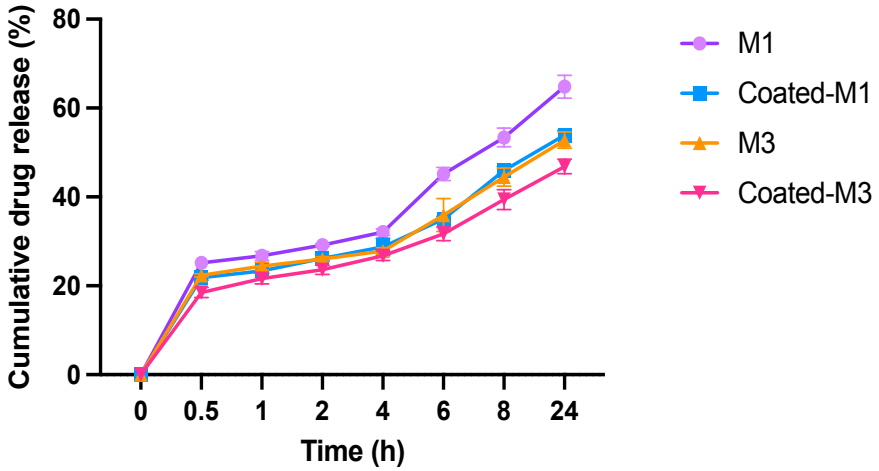


**Fig. 2: In-vitro release profiles of ORZ from uncoated micelle-core formulae (M1 and M3) and chitosan coated micelles (C-M1$_{(0.5)\ and}$ C-M13$_{(0.5)}$) in simulated intestinal fluid at 37 °C.**

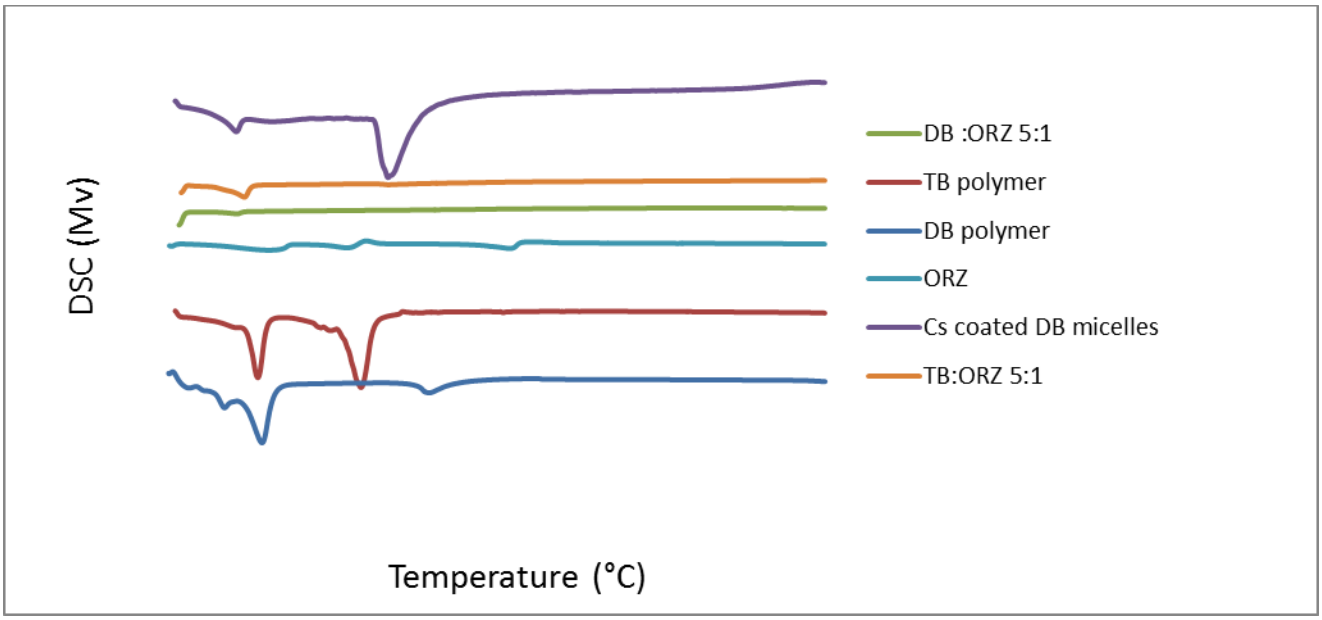


**Fig. 3: DSC thermograms of ORZ, DB, TB copolymers, uncoated micelles (M1 and M3) and chitosan coated micelles (C-M1$_{(0.5)}$ and C-M13$_{(0.5)}$).**

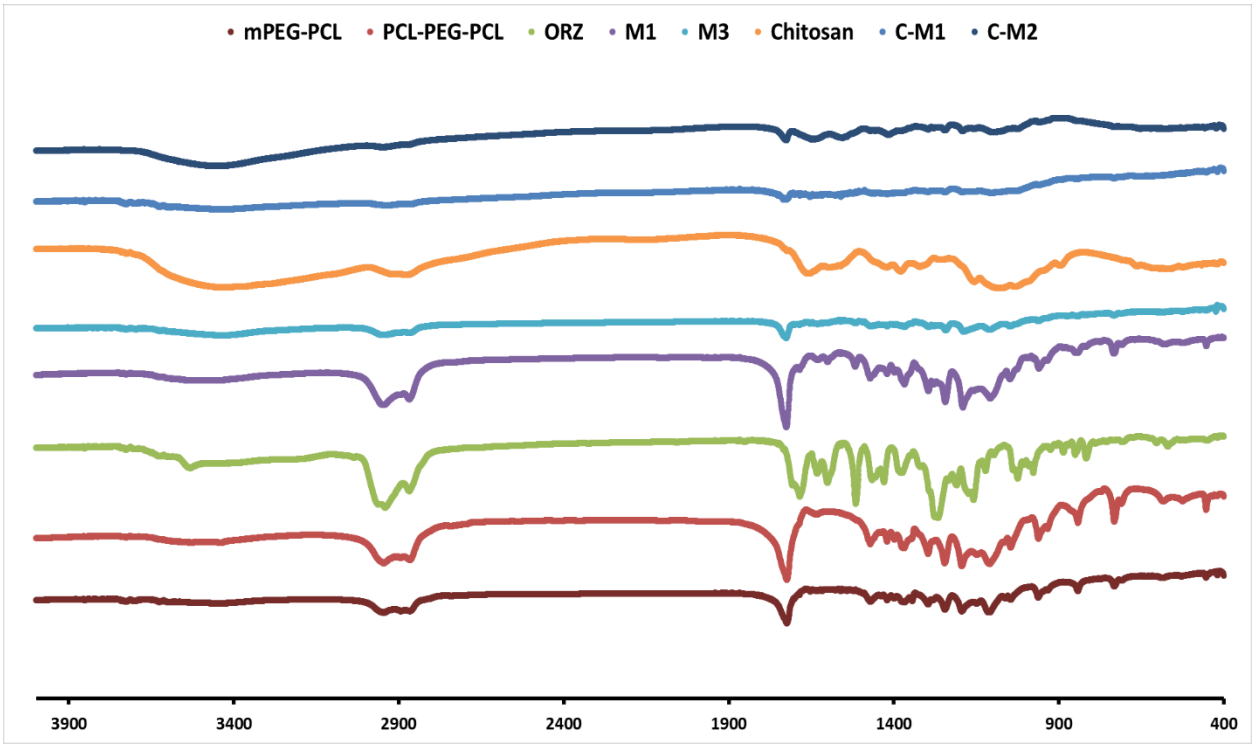

**Fig.4: FTIR spectra of ORZ, DB, TB copolymers, uncoated micelles (M1 and M3) and the chitosan coated micelles (C-M1$_{(0.5)\ and}$ C-M3$_{(0.5)}$).**

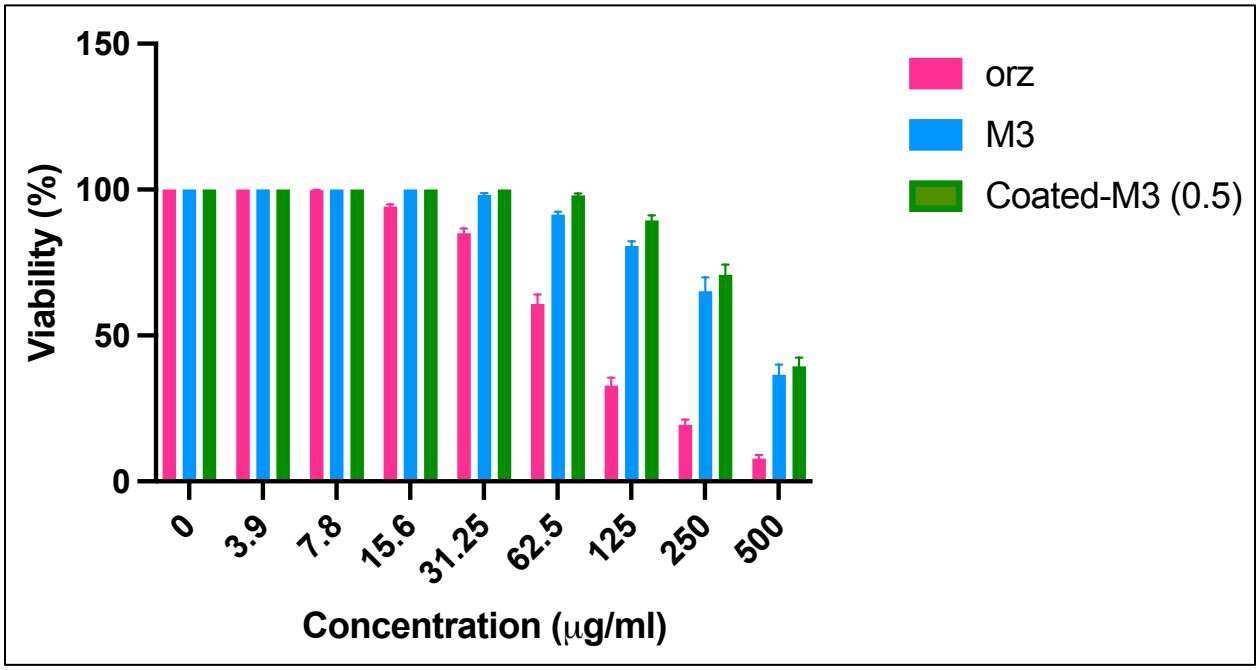


**Fig 5: Percent cell viability of Vero cells after 24 h incubation with free ORZ , uncoated micelles (M3) and chitosan coated micelles ( C-M13$_{(0.5)}$)**

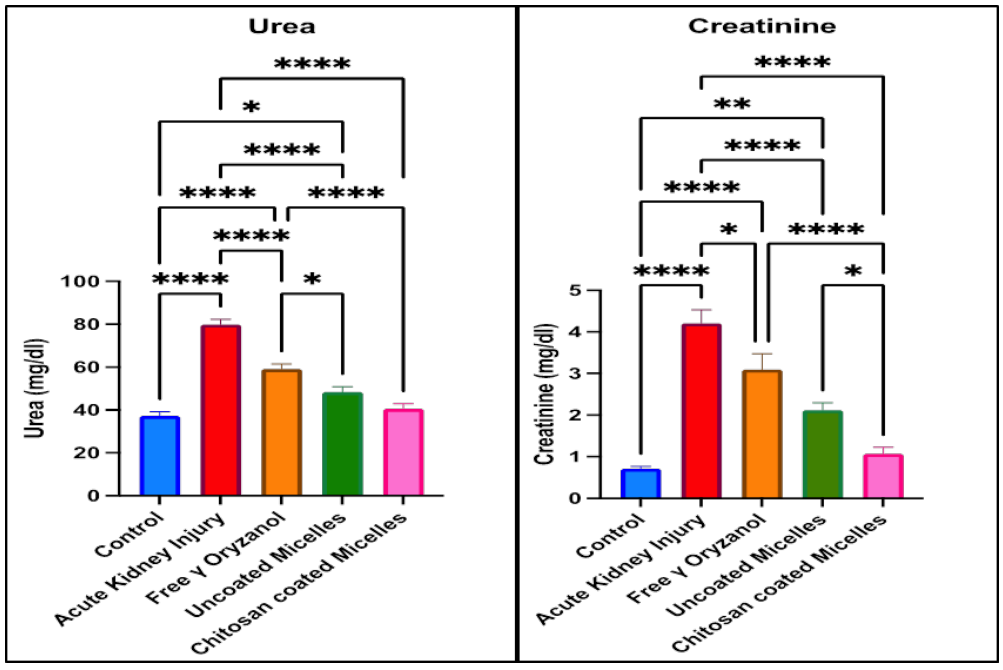

**Fig 6: Nephrotoxic indices; a) urea and b) creatinine of the different rat groups following in glycerol induced AKI model.** ***Uncoated micelles (M3) and Corresponding chitosan coated micelles ( C-M3$_{(0.5)}$)***

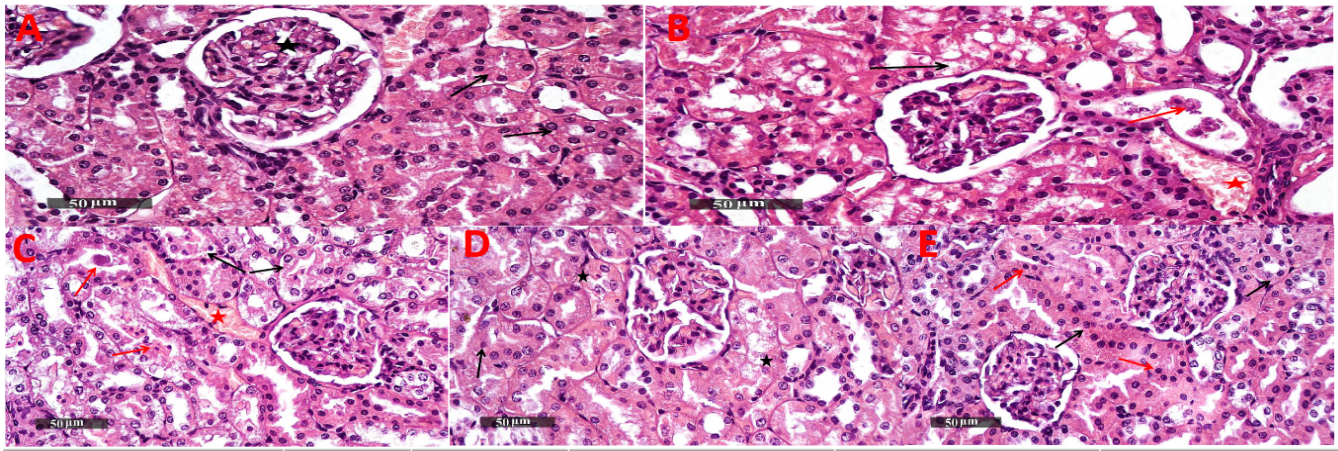


| F | Control (A) | AKI (B) | Free γ Oryzanol (C) | Uncoated Micelles (D) | Chitosan coated γ Oryzanol (E) |
|---|---|---|---|---|---|
| Congested blood vessels | 0 | 2 | 2 | 0 | 0 |
| Tubular necrosis | 1 | 4 | 3 | 2 | 1 |
| Luminal casts | 0 | 4 | 2 | 2 | 1 |
| Cystic dilatation | 0 | 2 | 1 | 0 | 0 |

**Figure 7: Effects of free, chitosan coated and uncoated ORZ treatment on renal histopathology and scoring in glycerol induced acute kidney injury.**

**Photomicrographs of H&E stained sections of kidney depicting (A) Control group shows normal histological features of renal parenchyma with apparent intact renal corpuscles (star), renal tubular segments with almost intact tubular epithelium (arrow) as well as intact vasculatures.(B) Glycerol induced AKI shows sever alteration of histological features than control group with more abundant records of necrotic and hyperesenophilic tubular segments losing its luminal border integrity (black arrow) as well as moderate cystic dilatation of some tubules higher records of intraluminal desquamated epithelial cells as well as casts were shown (red arrow) and mild congested interstitial blood vessels (red star).(C) Free ORZ group shows diffuse records of moderate tubular degenerative changes with many figures of vacuolar degeneration of various tubular segments (black arrow) with occasional necrotic cells, mild focal records of intraluminal cellular casts (red arrow) and mild congested interstitial blood vessels (red star).(D) Uncoated micelle group shows mild protective efficacy with moderate higher records of tubular vacuolar degenerative changes (arrow) with few focal records of tubular necrosis (star). (E) Chitosan coated micelles group of ORZ demonstrates mild focal records of tubular degenerative changes and nuclear pyknosis(red arrow) with abundant records of apparent intact nephronal segments (black**

**arrow) and renal corpuscles with intact vasculatures.(F) Renal damage score in different studied groups.** ***Uncoated micelles (M3) and Corresponding chitosan coated micelles ( C-M3$_{(0.5)}$)***

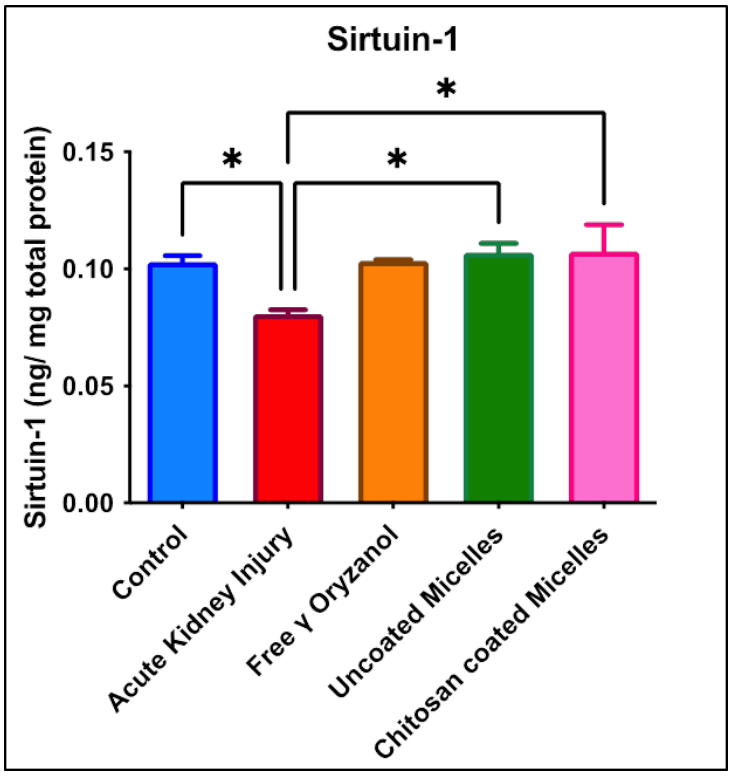


**Figure 8: Effects of free ORZ , uncoated and chitosan coated ORZ treatment on renal sirtuin -1 levels in glycerol induced acute kidney injury. Data are presented as mean ± SEM (n = 4). Statistical Analysis was performed using one-way ANOVA followed byTukey's test as post-hoc test.** ***Uncoated micelles (M3) and Corresponding chitosan coated micelles ( C-M3$_{(0.5)}$)***

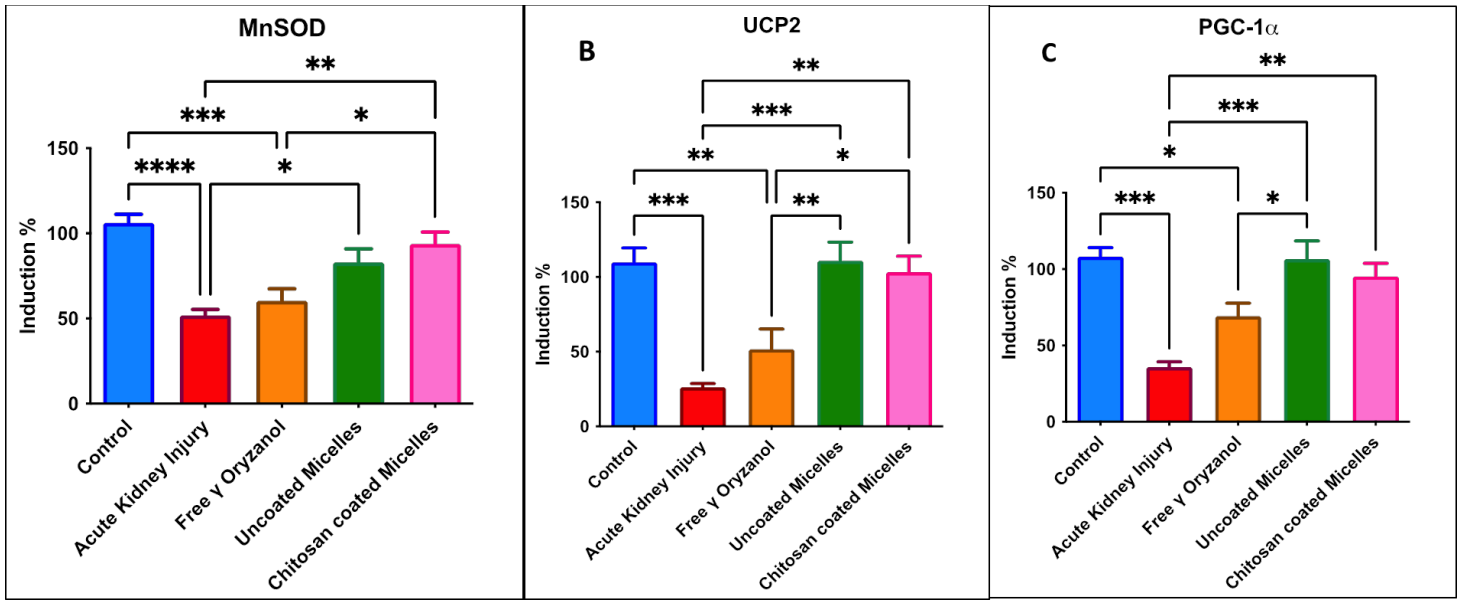


**Figure 9: Effects of free ORZ, chitosan coated and uncoated micleestreatmenton renal expression ofantioxidant genes: (A) MnSOD, (B) UCP2 and (C) PCG-1α in glycerol induced acute kidney injury. Data are presented as mean ± SEM (n = 4). Statistical Analysis was performed using one-way ANOVA followed by Tukey's test as post-hoc test.**

***Uncoated micelles (M3) and Corresponding chitosan coated micelles ( C-M3$_{(0.5)}$)***

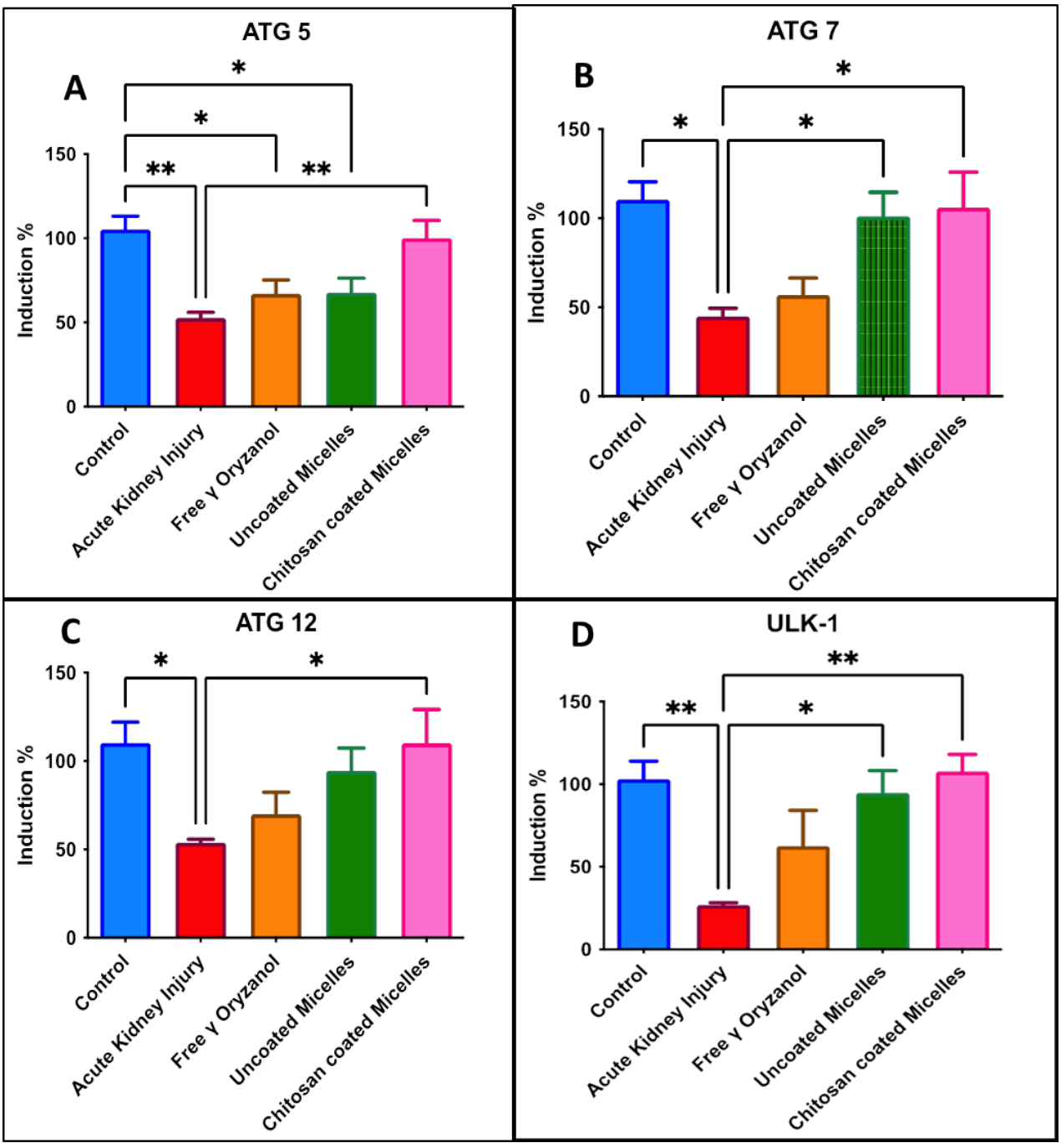


937

938 **Figure 10: Effects of free ORZ, uncoated and chitosan coated ORZ treatment on renal**
939 **expression of autophagy genes: (A) ATG 5, (B) ATG 7, (C) ATG 12 and (D) ULK-1in**
940 **glycerol induced acute kidney injury. Data are presented as mean ± SEM (n = 4). Statistical**
941 **Analysis was performed using one-way ANOVA followed by Tukey's test as post-hoc test.**
942 ***Uncoated micelles (M3) and Corresponding chitosan coated micelles ( C-M3$_{(0.5)}$)***

943 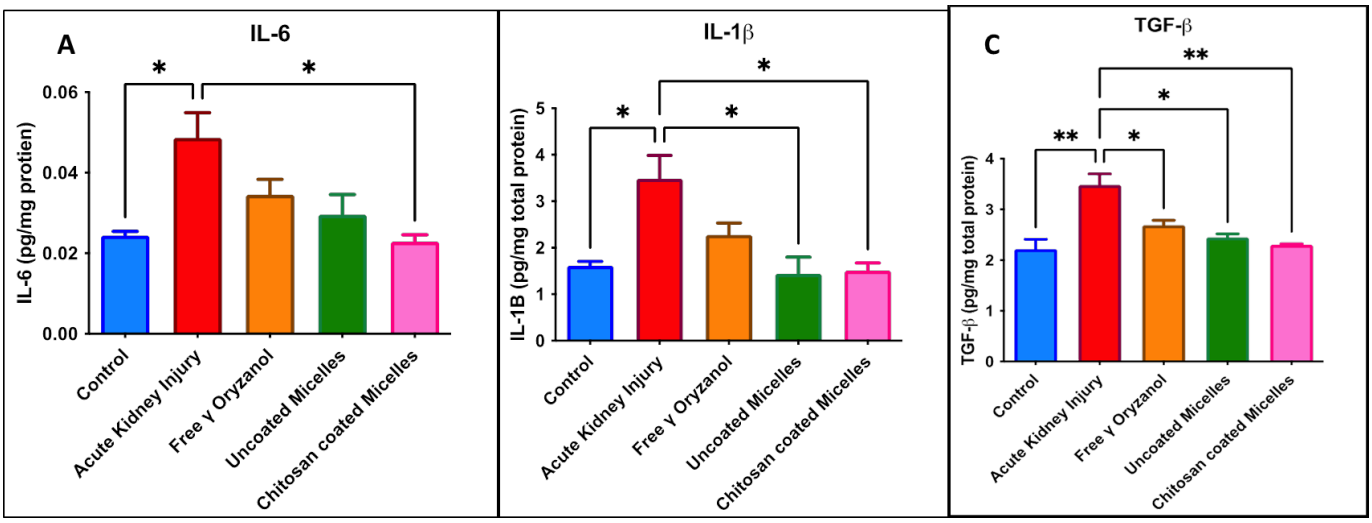


944 **Figure 11: Effects of free ORZ, uncoated and chitosan coated γ oryzanol treatment on**
945 **renal inflammatory markers: (A) IL-6, (B) IL-1βand (C) TGF-βin glycerol induced acute**
946 **kidney injury. Data are presented as mean ± SEM (n = 4). Statistical Analysis was**
947 **performed using one-way ANOVA followed by Tukey's test as post-hoc test.**

948 ***Uncoated micelles (M3) and Corresponding chitosan coated micelles ( C-M3$_{(0.5)}$)***

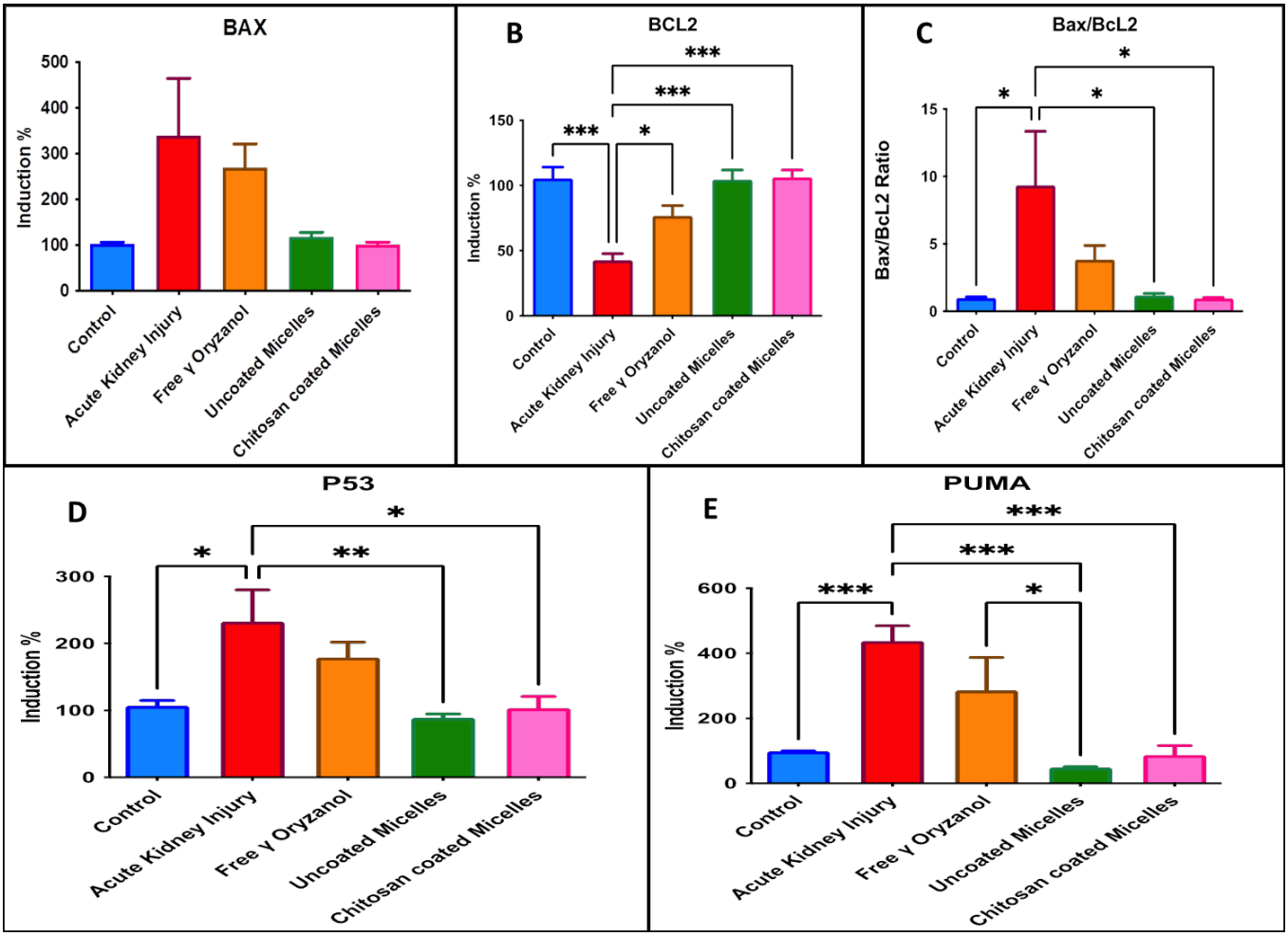


**Figure 12: Effects of free ORZ, uncoated and chitosan coated ORZ treatment on renal expression ofapoptotic genes: (A) BAX, (B) BcL-2, (C) BAX/BcL2 ratio, (D) P53 and (E) PUMA in glycerol induced acute kidney injury. Data are presented as mean ± SEM (n = 4). Statistical Analysis was performed using one-way ANOVA followed by Tukey's test as post-hoc test.** ***Uncoated micelles (M3) and Corresponding chitosan coated micelles ( C-M3$_{(0.5)}$)***

**Table 1: Fabrication,colloidalparameters, drug loading levels and encapsulation efficiencies of ORZ micelle-core (each value represents the mean±SD, *n* = 3).**

| Formulation | Copolymer type | Polymer ratio to ORZ | PS (nm) | PDI | ZP (mV) | DL (%) | EE (%) |
|---|---|---|---|---|---|---|---|
| **M1** | DB | 5 to 1 | 105.4 ±0.87 | 0.255 ±0.012 | -12.6 ±2.1 | 13.45 ±0.99 | 67.28 ± 4.98 |
| **M2** | DB | 10 to 1 | 98.88 ±0.461 | 0.219 ±0.003 | -14.4 ±0.643 | 7.93 ±0.17 | 79.34 ±1.77 |
| **M3** | TB | 5 to 1 | 117.8 ±0.945 | 0.249 ±0.017 | -27.8 ±1.76 | 17.00 ±0.63 | 85.03 ±3.17 |
| **M4** | TB | 10 to 1 | 97.9 ±11.22 | 0.381 ±0.077 | -29.2 ±2.54 | 9.38 ±0.21 | 93.87 ±2.10 |

980

981 **Table 2**: **Sequences of primers pairs used for gene expression analysis.**

982

| **Gene symbol** | **Primer sequence** |
|---|---|
| MnSOD F: | 5′-GTGCAGGTAAGTGGCAGGG -3′ |
| MnSOD R: | 5′-TCGTGGTACTTCTCCTCGGT -3′ |
| UCP2 F: | 5′-CGTCTGCACTCCTGTGTTCT-3′ |
| UCP2 R: | 5′-TGTTGAGTGGGGCATTGTGT -3′ |
| PGC-1α F: | 5'-AGCCTCTTTGCCCAGATCTT-3' |
| PGC-1α R: | 5'-GCAATCCGTCTTCATCCACC-3' |
| ATG 5 F: | 5'-TGGACCATCAACCGGAAACT-3' |
| ATG 5 R: | 5'-AAGGGTATGCAGCTGTCCAT-3' |
| ATG 7 F: | 5'-CTGCTCTCGAAAACCCCATG-3' |
| ATG 7 R: | 5'-AAGAAGTATGGCAGGGCTGT-3' |
| ATG 12 F: | 5'-CTCTCCCCAGAAACAGCCAT-3' |
| ATG 12 R: | 5'-TCGATGAGTGCTTGGACAGT-3' |
| ULK1 F: | 5'-GTTGCTGACTCCAAGCCAAA-3' |
| ULK1 R: | 5'-ATCTTGGAGGACGAAAGCCA-3' |
| Bax F: | 5′-GATCAGCTCGGGCACTTTA-3′ |
| Bax R: | 5′-TGTTTGCTGATGGCAA CTTC-3′ |
| Bcl-2 F: | 5′-AGGAT TGTGG CCTTC TTTGA GT-3′ |
| Bcl-2 R: | 5′-GCCG GTTC AGG TACT CAGT CAT-3′ |
| Tp53 F: | 5′-CAGCTTTGAGGTTCGTGTTTGT-3′ |
| Tp53 R: | 5′-ATGCTCTTCTTTTTTGCGGAAA-3′ |
| PUMA F: | 5′-GTG TGG AGG AGGAGG AGT GG-3′ |
| PUMA R: | 5′-TCG GTG TCG ATG TTG CTC TT-3′ |
| β-actin F: | 5′- TGTCACCAACTGGGACGATA-3′ |
| β-actin R: | 5′- GGGGTGTTGAAGGTCTCAAA-3′ |

MnSOD, manganese superoxide dismutase; UCP2, uncoupling protein-2; PGC-1α, Peroxisome proliferator-activated receptor gamma coactivator 1-alpha; ATG, Autophagy-related genes; ULK1, unc-51 like autophagy activating kinase 1; Bax, Bcl-2-associated X protein; Bcl-2, B-cell lymphoma2; Tp53, tumor protein 53; PUMA, p53 upregulated modulator of apoptosis; β-actin, beta actin.

**Table 3: Fabrication and colloidal parameters of ORZ chito-micelles (each value represents the mean±SD, *n* = 3).**

| Formulation | CS concentration | PS (nm) | PDI | ZP (mV) |
|---|---|---|---|---|
| **M1** | - | 105.4±0.87 | 0.255±0.012 | -12.6±2.1 |
| **C-M1$_{(0.25)}$** | 0.25 | 136.7±7.605 | 0.393±0.021 | 23.2±1.56 |
| **C-M1$_{(0.5)}$** | 0.5 | 178.5±4.424 | 0.458±0.033 | 31.5±2.95 |
| **C-M1$_{(1)}$** | 1 | 411±12.75 | 0.61±0.153 | 41.8±1.99 |
| **M3** | - | 117.8±0.945 | 0.249±0.017 | -27.8±1.76 |
| **C-M3$_{(0.25)}$** | 0.25 | 156.9±1.47 | 0.41±0.063 | 24.9±2.24 |
| **C-M3$_{(0.5)}$** | 0.5 | 194.8±1.185 | 0.428±0.003 | 37.4±0.781 |
| **C-M3$_{(1)}$** | 1 | 480±10.68 | 0.927±0.023 | 44.1±0.850 |

**Table 4: Stability of Optimized ORZ-loaded chito-micelles after 1-month and 3-month storage periods at room temperature and 4°C**

| **Parameter** | **Fresh C-M3$_{(0.5)}$** | **Stored C-M3$_{(0.5)}$ at 4°C** | | |
|---|---|---|---|---|
| | | 7 days | 14 days | 28 days |
| PS (nm) | 194.8±1.185 | 190.5±7.65 | 210.9±5.26 | 213.9±9.27 |
| PDI | 0.42±0.003 | 0.48±0.01 | 0.42±0.009 | 0.43±0.03 |
| ZP (mV) | 37.4±0.781 | 37.8±1.2 | 36±2.32 | 33.2±0.89 |